

UC Davis

UC Davis Previously Published Works

Title

Engineered channel controls limiting spawning habitat rehabilitation success on regulated gravel-bed rivers

Permalink

<https://escholarship.org/uc/item/90g5t0dr>

Journal

Geomorphology, 97(3-4)

ISSN

0169555X

Authors

Brown, Rocko A
Pasternack, Gregory B

Publication Date

2008-05-01

DOI

10.1016/j.geomorph.2007.09.012

Peer reviewed

1 **Engineered channel controls limiting spawning habitat rehabilitation success on regulated**
2 **gravel-bed rivers**

3

4 Rocko A. Brown and Gregory B. Pasternack*

5

6

7

8 Department of Land, Air, and Water Resources, University of California, One Shields Avenue,

9 Davis, CA 95616, USA.

10

11

12 *Corresponding author. Tel.: +530-754-9243; E-mail: gpast@ucdavis.edu

13

14

15

16

17

18

19

20

21

22

23

24 **Abstract**

25 In efforts to rehabilitate regulated rivers for ecological benefits, the flow regime has been one of
26 the primary focal points of management strategies. However, channel engineering can impact
27 channel geometry such that hydraulic and geomorphic responses to flow reregulation do not
28 yield the sought for benefits. To illustrate and assess the impacts of structural channel controls
29 and flow reregulation on channel processes and fish habitat quality in multiple life stages, a
30 highly detailed digital elevation model was collected and analyzed for a river reach right below a
31 dam using a suite of hydrologic, hydraulic, geomorphic, and ecological methods. Results
32 showed that, despite flow reregulation to produce a scaled-down natural hydrograph,
33 anthropogenic boundary controls have severely altered geomorphic processes associated with
34 geomorphic self-sustainability and instream habitat availability in the case study. Given the
35 similarity of this stream to many others, we concluded that the potential utility of natural flow
36 regime reinstatement in regulated gravel-bed rivers is conditional on concomitant channel
37 rehabilitation.

38

39

40 Keywords: river restoration; fluvial geomorphology; flow reregulation; two-dimensional
41 modeling; salmonid habitat

42

43

44

45

46 **1. Introduction**

47

48 Alluvial rivers consist of a geometric channel with bank and bed boundaries over which
49 the inputs of water and sediment pass creating a suite of physical processes (Leopold et al.,
50 1964). Thus, the physical controls for a river may be distinguished as boundary or input related
51 (Table 1). Each of these can be further subdivided into natural or anthropogenic in origin, and
52 each has a spatiotemporal range of influence. Most research on the effects of dams and on
53 methods for restoring regulated rivers have emphasized manipulation of the input regime, with
54 the assumption that boundary changes will follow from reregulation, just as natural channel
55 change stems from natural input changes (Graf, 1996; Poff et al., 1997). However, in natural
56 systems, no anthropogenic boundary controls exist, so the flow regime is effective at achieving
57 channel change (Parker et al., 2003). The overall goal of this study was to evaluate the
58 constraints imposed by anthropogenic boundary controls on the potential benefits of flow
59 reregulation for rehabilitating a regulated river in a typical constrained reach below a major dam.
60 Flow reregulation is defined as increases in the magnitude and duration of water releases below
61 dams timed to achieve key ecological and geomorphic functions, such as promoting successful
62 anadromous fish spawning and rejuvenating gravel-bed features during spring flow pulses.
63 Impacts are defined in terms of the regulated channel's hydraulic, sediment transport, and
64 physical habitat regimes at the hydraulic unit and geomorphic unit spatial scales, as defined next.
65 The significance of this study is that it illustrates how existing physical constraints can limit the
66 potential for flow reregulation to promote river rehabilitation.

67

68 *1.1. Physical controls*

69 Input controls are those that affect the river's flow and sediment supply regimes. Natural
70 "genetic" controls include topography, geology, climate, soils, and vegetation, with the
71 topographic variables of upslope contributing area and local slope providing a particularly strong
72 influence on landscape processes (Montgomery 1999; Montgomery and Buffington, 1997;
73 Montgomery et al., 1996). Anthropogenic input controls include land use, dams, and diversions.
74 Land use affects the gross supply of water and sediment to streams (Bosch and Hewlett, 1982;
75 Jacobson, 1995; Pasternack et al., 2001; Constantine et al., 2005), whereas dams and diversions
76 determine the timing, magnitude, frequency, and rate of change of delivery of inputs to
77 downstream areas (Williams and Wolman, 1984; Kondolf, 1997; Grant et al., 2003).

78 Boundary controls primarily affect fluvial processes at the hydraulic unit (10^1 - 10^0
79 channel widths) and geomorphic unit (10^1 channel widths) scales and are typically limited to the
80 reach (10^2 - 10^3 channel widths) in which they occur. Boundary controls affect channel structure
81 and mediate the response of the channel to flow regime impacts by directing or restricting
82 channel change (Lisle, 1986; Abbe and Montgomery, 1996; Thompson et al., 1998; USFWS,
83 1999). As a boundary control, valley confinement and valley width variation affects many
84 gravel-bed rivers (Jacobson and Gran, 1999; Coulombe-Pontbriand and Lapointe, 2004).
85 Compared to unconfined channels, the hydraulics of valley-confined channels tend to
86 concentrate flow and bed shear stress in a channel's center with increasing discharge, creating
87 reaches with high transport capacity (Leopold et al., 1964; McBain and Trush, 2000; Constantine
88 et al., 2003). The persistence of pool and riffle sequences has also been related to boundary
89 controls such as bedrock outcroppings, bar features, logjams, and valley geometry (Lisle, 1986;
90 Thompson et al., 1998; MacWilliams et al., 2006). Large changes in relative cross-sectional area
91 between pools and riffles as a function of discharge yield hydraulic "reversals" in which velocity

92 and bed shear stress are greater for riffles than pools at low discharge, but then are greater for
93 pools than riffles at high discharge (Keller, 1971; Carling, 1991; Thompson et al., 1998;
94 MacWilliams et al., 2006).

95 Anthropogenic boundary controls occur at subreach spatial scales and involve direct
96 channel interventions (Table 1). Because anthropogenic boundary controls generally constrict
97 channels and reduce their roughness (Erskine, 1992; Surian and Rinaldi, 2003), they increase
98 transport capacity and decrease physical-habitat diversity, reducing ecological productivity and
99 diversity (Negishi et al., 2002; Merz et al., 2004; Merz and Ochikubo Chan, 2005). Bed
100 armoring, vegetation encroachment, and levee formation can indirectly result from flow
101 regulation (Williams and Wolman, 1984; Kondolf, 1997; USFWS, 1999). Although such input
102 alterations cause these boundary controls, the effect of these boundary controls is on the
103 boundary and thus its designation as an anthropogenic boundary control. Bank stabilization is
104 used to prevent channel migration and reduce bank erosion that produces sand, silt, and clay
105 (Chang, 1988). Engineered in-stream structures also exist to constrain or aid channel dynamics
106 in association with dams, check dams, bed sills, artificial riffles, boulder clusters, and wood
107 (Abbe et al., 2003; Cederholm et al., 1997; Newbury et al., 1997; Thompson and Stull, 2002).
108 In-stream structures may be used to promote fluvial diversity in support of ecological health
109 (Hunter, 1991; Thompson and Stull, 2002; Wheaton et al., 2004c, Elkins et al., 2007). Artificial
110 riffles are frequently prescribed for slope control and consist of weir like arrangements of large
111 boulders (0.5-2.0 metric ton) that are often cabled (Thompson, 2002; Saldi-Caromile et al.,
112 2004).

113

114 *1.2. Study objectives*

115 While there is literature discussing flow reregulation for improving streams (e.g., Poff et
116 al., 1997; Webb et al., 1999; Galat and Lipkin, 2000), the consequence of not addressing
117 anthropogenic boundary controls when considering flow reregulation has not been carefully
118 weighed. This research examines the potential for salmonid habitat rehabilitation by flow
119 reregulation alone for a reach directly below a dam on a midsized regulated gravel-bed river that
120 has experienced numerous channel engineering measures. Two types of boundary controls
121 (anthropogenic valley confinement and artificial riffles) are examined to determine their affect
122 on channel response to increased discharge with respect to hydraulic variables (i.e., depth and
123 velocity), sediment transport regime, and physical habitat of salmonids. The impacts associated
124 with these specific controls are important because they are frequently prescribed and
125 implemented in channel engineering and restoration efforts.

126

127 **2. Study site**

128

129 *2.1. Trinity River basin*

130 The Trinity River above Lewiston, CA, is a 1860-km² basin (Fig. 1) that is part of the
131 Klamath Mountain Province in northwestern California. It has a high point of over 2700 m, and
132 the terrain is steep with deep gorges. The basin is far enough inland to have extreme weather
133 variations, with winter snows and hot, dry summers. Average annual precipitation ranges from
134 90-190 cm. Natural streamflow is governed by large winter storms (October to March) and
135 moderate spring snowmelt.

136 The Trinity Dam was built in 1962, with Lewiston Dam built shortly after and 13 km
137 downstream the valley. Peak flows at the Lewiston Dam site reached as high as 2100 m³/s prior

138 to damming (Fig. 2). From 1962-1979, up to 90% of the total inflow was diverted to the
139 Sacramento River basin. From 1979-2004, diversions were reduced to 75%. Recent legislation
140 has now restricted total diversions to 53%.

141 Damming of the Trinity River altered channel morphology in several ways. The
142 reduction in coarse sediment has led to monotypic morphologies characterized by glides with
143 high velocities (USFWS, 1999). The reduction in both the frequency and magnitude of floods
144 has allowed riparian vegetation to encroach channel margins, creating riparian berms and
145 fossilizing gravel bars. This confinement increases bed shear stress through the channel
146 centerline with increasing discharge. Over time, this has led most reaches to develop a
147 symmetric, trapezoidal cross section. Loss of asymmetry has decreased habitat diversity, such
148 that shallow water habitat occurs only on channel margins and is eliminated at intermediate
149 discharges between 11-57 m³/s (USFWS, 1999).

150 The Trinity River supports 18 fish species, including eight anadromous ones: chinook
151 salmon, chum salmon, coho salmon, steelhead trout, American shad, green sturgeon, speckled
152 dace, and Pacific lamprey. Damming has affected fisheries habitats on the Trinity River by
153 blocking over 160 km of upstream spawning grounds and by reducing instream flows necessary
154 to flush sand and drive geomorphic processes that maintain alluvial spawning grounds. The
155 culmination of dam effects on anadromous fish has been devastating, resulting in 80-90% loss of
156 salmonid habitat by 1980 (USFWS, 1999). Chinook and coho salmon as well as steelhead trout
157 have experienced losses of 67, 96, and 53% of pre-dam averages, respectively, and consequently
158 these species are the focus of restoration efforts. Historically, an average of 66,000 chinook,
159 10,000 steelhead, and 5,000 coho adults migrated past Lewiston each year. Spawning between
160 the three species was distributed with channel gradient, with coho and steelhead spawning in

161 upper headwaters and chinook spawning in the mainstem and tributaries. Superposition of redds
162 is now more common as all three species reach the Lewiston dam with little available space for
163 spawning. The target for a fall-run chinook salmon population is 62,000 (nonhatchery fish).
164 Most spawning occurs in a 3.3-km reach below the Lewiston Dam (USFWS, 2002). Fisheries
165 populations are enhanced by hatchery fish that supplement post-dam in-river escapement of fall-
166 run chinook, spring-run chinook, coho, and fall-run steelhead by 56, 68, 97, and 30%
167 respectively. River rehabilitation activities on the Trinity River include gravel augmentation,
168 channel reconfiguration, bank vegetation removal, and flow reregulation below Lewiston Dam
169 (USFWS, 1999).

170

171 2.2. *Lewiston hatchery reach*

172 The 760-m Lewiston hatchery reach (LHR) is located immediately downstream of
173 Lewiston Dam (Fig. 2; 40°43'34"N, 122°47'48"W) and is the uppermost limit of spawning access
174 on the Trinity River. Historically, the reach was characterized by a wide channel with inset
175 active alluvial gravel bars and a wide forested floodplain (Fig. 3A). Valley walls on river right
176 served as a limiting boundary control on channel adjustment. Channel width was otherwise free
177 to adjust to changes in discharge and sediment supply. A deep constricted pool is evident in the
178 photo followed by a diverging alluvial transverse bar feature. The alluvial transverse bar most
179 likely provided hydraulic diversity that provided habitat for a multitude of species and life stages
180 of salmonids. This large riffle feature began at a bedrock-induced constriction. As sediment was
181 routed through the deep and constricted upstream pool, the expansion following the bedrock
182 outcrop likely reduced velocities and promoted settling of entrained sediments.

183 Currently, the LHR has three types of boundary controls: armoring induced by the dam,
184 anthropogenic valley confinement, and artificial riffles that cannot be self-adjusted under the
185 current flow regime. The reach is artificially straight confined on the river left by the Lewiston
186 Hatchery on the river right by the valley walls (Figs. 2B, 4A). The left bank is confined by
187 floodplain infill placed during construction of the Lewiston Hatchery and are sloped
188 approximately uniform at 45° and consist of 1 to 2 metric-ton rocks. In comparing the present
189 conditions with a 1939 United States Geological Survey topographic map (1:31680 scale with a
190 contour interval of 6.1 m contour), channel width has been decreased by as much as 40%.
191 Channel width ranges from 24-46 m at 8.5 m³/s (the regulated spawning-period discharge). The
192 right bank is confined by the valley wall with steep banks, > 10%, composed of bedrock outcrop,
193 thin soils, and sparse vegetation. Because of its position in the basin and associated high rate of
194 bed material export, the LHR has been a primary location for gravel augmentation (USFWS,
195 1999; Kondolf and Minear, 2004; Wilcock, 2004). Since 1972, there have been numerous gravel
196 enhancement projects below Lewiston Dam resulting in the addition of over 27,370 m³ of gravel
197 and large boulders (Kondolf and Minear, 2004). Within the LHR, there are four riffles, three of
198 which are artificial, “rock-weir” riffles composed of coarse cobbles and boulders remaining from
199 past gravel augmentation and slope control projects (Figs. 2B, 4B). Riffles 1, 2, and 4 were
200 constructed in 1976. They were built to stabilize the existing longitudinal profile. In 1983,
201 4,128 m³ were added to riffle 3. The only “natural” riffle is located near a fishing access point.
202 This one may be self-formed, because there are no records of gravel placement at this location.
203 Also, a bedrock outcrop between riffles 2 and 3 induces a visible flow convergence at 8.5 m³/s.
204 As a consequence of relatively frequent construction activities, all artificial riffles have
205 compacted gravel protrusions into the channel. These constrictions, along with the valley and

206 hatchery confinement, effectively have made the riffles narrower than the pools, thereby likely
207 focusing high velocities and scour at those locations. Three outfall pipes from the adjacent
208 hatchery are within the study reach. These outfall pipes have created highly localized scour
209 holes, but do not produce significant discharge relative to the dam releases. Each of the
210 anthropogenic boundary controls acts hierarchically on different spatial scales. The rocky banks
211 of the Lewiston Hatchery, moderate bed slope, and narrow V-shaped valley are the primary
212 reach-scale controls. Geomorphic unit controls consist of fixed rocky banks, artificially cabled
213 rock riffles, and a bedrock constriction. Hydraulic unit controls include the outfalls from the
214 hatchery, the rock-weir riffles, gravel augmentation deposits, and the hatchery terrace
215 confinement.

216

217 **3. Methods**

218

219 To evaluate the effectiveness of flow reregulation in the LHR a combination of empirical,
220 analytical, and numerical methods were used to determine the impact of anthropogenic boundary
221 controls on salmonid rehabilitation. The impact of anthropogenic boundary controls on reach
222 and geomorphic unit scale hydraulic and geomorphic processes was evaluated by using
223 longitudinal profile and hydraulic-geometry analyses. Long-profile analysis can allow
224 determination of dominating factors controlling slope distribution. Cross-sectional hydraulic
225 geometry can be used to analyze channel response to flow reregulation over a wide range of
226 discharges beyond that observed during the study period. Geomorphic unit self-sustainability of
227 the riffles and pools present in the LHR was evaluated by comparing log-log plots of velocity
228 versus discharge for riffle and pool sections to discern the presence of a hydraulic reversal

229 mechanism in the reach associated with relative cross-sectional area (Keller, 1971; MacWilliams
230 et al., 2006).

231 Two-dimensional (2D) depth-averaged computational modeling was done to estimate
232 channel hydrodynamics, sediment transport regime (defined in terms of a range of Shields stress
233 values), and anadromous fish habitat patterns at the 1-m spatial scale relevant to key geomorphic
234 and ecologic functions of the channel. Quantitative analyses necessitated development of a high-
235 resolution digital elevation model (DEM) as well as gathering hydraulic and bed material data.
236 The 2D model node values of depth and velocity for each discharge evaluated were plotted to
237 analyze trends in hydraulic distribution with increasing stage. The flow release regime for
238 Lewiston Dam was used to select appropriate discharges for assessing the impact of boundary
239 controls on key ecological and geomorphic processes. The discharges studied were the autumnal
240 anadromous fish spawning flow (8.5 m³/s), late summer adult fish holding flow (13 m³/s), early
241 summer anadromous fish attraction flow (70.8 m³/s), and the peak dam release during the study
242 (170 m³/s). These flows are re-regulated releases from Lewiston Dam associated with the effort
243 to provide a more natural flow regime. Floodplain structures and bridges prevent any
244 substantially higher peak releases from occurring in the near future.

245

246 *3.1. Field methods*

247 A detailed topographic survey was conducted using a Topcon GTS-802A robotic total
248 station in summer 2003 yielding 15,284 points from the bed, boulders, edge of water, and water
249 surface elevation within the 13 m³/s channel. A standard feature-based surveying method was
250 used (Wheaton et al., 2004b) yielding a sampling density of 1.3 pts/m². Water surface elevations
251 along the study reach were measured at 8.5, 13, 127.4, and 170 m³/s relative to the NAVD88

252 vertical datum. Geomorphic features within the study reach were identified, surveyed, and
253 incorporated into the DTM.

254 Fourteen cross sections were selected to characterize the geomorphic unit variations in
255 the LHR (Fig. 5). Wolman pebble counts (Wolman, 1954) were performed on cross sections 1,
256 2, 3, 4, 10, 11, 13, and 14. Grain size distributions were calculated for each cross section and
257 averaged for the project reach. Velocity validation measurements were recorded at cross
258 sections 1, 2, 3, 13, and 14 at a discharge of $13 \text{ m}^3/\text{s}$. Flow conditions were too dangerous to
259 obtain velocity data at the highest discharges. Cross section endpoints were surveyed with the
260 Topcon GTS-802A so that field data could be compared to model predictions for the same
261 location. Depth and velocity were measured at 1.5 m intervals between surveyed endpoints. A
262 Marsh-McBirney Flo-mate ($\pm 33 \text{ mm/s}$) mounted to a depth setting wading rod was used to
263 estimate average velocity as the point velocity at 0.6·depth, because the water was shallow
264 (Pasternack et al., 2006). Positional accuracy and observation resolution was much finer than the
265 scale of bed features (5-10 m) and similar to 2D model node spacing.

266 3.2. *Digital elevation model*

267 A DEM of the study reach was constructed using the surveyed topographic points in
268 Autodesk, Land Desktop 3. The four iterative stages of DEM development as described by
269 French and Clifford (2000) were implemented: interpolation, visualization, editing, and
270 augmentation. First, survey data were interpolated and a surface defined respecting breaklines.
271 Next, the surface was visualized as a map and edited to remove obvious interpolation errors. The
272 revised surface was visually verified in the field to check for poorly represented areas in the
273 DEM. Further iteration was done as needed. All 14 cross sections and a thalweg profile were
274 extracted from the DEM using Land Desktop. At each cross section, mean depth, top width of

275 flow, width-to-depth ratio, wetted perimeter, hydraulic radius, and area were calculated at 0.3-m
276 intervals from the 8.5 m³/s water surface elevation to a water surface elevation 4 m above.

277

278 3.3. Hydraulic geometry analysis

279 Boundary controls have been noted to have an impact on hydraulic geometry relations in
280 cases where channel width is constrained (Singh, 2003). Holding one variable relatively
281 constant (for example, channel width), the hydraulic response will be largely dictated by changes
282 in nonstatic variables such as depth and velocity, which may have an impact on geomorphic
283 processes such as riffle and pool sustainability, and thus spatial nested geomorphic features
284 necessary for salmonid fisheries. *Ceteris paribus*, unforced riffles and pools are considered
285 geomorphically self-sustainable over time if the local bed shear stress over pools exceeds that
286 over riffles at some discharge above bankfull so that the existing topographic variation is
287 maintained as long as sediment is supplied to the riffle-pool sequence (Keller, 1971; Carling,
288 1991; Clifford and Richards, 1992; Booker et al., 2001; MacWilliams et al., 2006). Cross-
289 sectional analyses of riffle-pool sustainability have yielded somewhat contrasting results
290 depending on the resolution of the tools used to study the phenomenon. If a hydraulic reversal is
291 present in mean flow variables, then it will also be present in local ones, though the converse is
292 not true (McWilliams et al., 2006). Thus, analysis of mean flow conditions is a conservative
293 predictor of riffle-pool sustainability. Cross sections were analyzed to estimate the effect of
294 increasing discharge and channel geometry on hydraulics and riffle-pool self-sustainability. At-
295 a-station hydraulic geometry equations (Leopold and Maddock, 1953) were used to develop
296 relationships between width, depth, and velocity as a function of discharge:

297

298
$$w = aQ^b, \quad \bar{H} = cQ^f, \quad \bar{U} = kQ^m \quad (1,2,3)$$

299

300 where w is top width (m), \bar{H} is cross-sectionally averaged depth (m); \bar{U} is cross-sectionally
301 averaged velocity (m/s); a , c , and k are regression coefficients; and b , f , and m are regression
302 exponents. Steady, uniform flow was assumed for calculating mean velocity. Manning's
303 equation was coupled with the continuity equations to predict depth and velocity:

304

305
$$\bar{U} = \left(\frac{1}{n}\right)R^{2/3}S^{1/2} \quad \text{and} \quad Q = \bar{U} A \quad (4,5)$$

306

307 where R is hydraulic radius, A is cross-sectional area, n is Manning's roughness coefficient, and
308 S is slope. Manning's n was approximated as 0.043 based on roughness tables for a straight,
309 coarse gravel channel with no vegetation (McCuen, 1989) and past studies in this channel type
310 (Pasternack et al., 2004, 2006; Wheaton et al., 2004b). For each cross section, w , \bar{H} , A , and R
311 were obtained in AutoCad as described in the above section. A ternary diagram was constructed
312 to compare the width, depth, and velocity exponent values (b , f , and m). To test for riffle and
313 pool sustainability via a hydraulic reversal, log-log plots of velocity versus discharge were
314 constructed and compared for all riffle and pool units. Also, the velocity results from the 2D
315 model were examined for the existence of velocity reversals, as reported later.

316

317 *3.4. 2D Trinity model*

318 Two-dimensional hydrodynamic models have existed for decades and have been used to
319 study a variety of hydrogeomorphic processes (Bates et al., 1992; Leclerc et al., 1995; Miller and

320 Cluer, 1998; Cao et al., 2003). Recently, they have been evaluated for use in regulated river
 321 rehabilitation emphasizing spawning habitat rehabilitation by gravel placement (Pasternack et al.
 322 2004, 2006; Wheaton et al. 2004b; Elkins et al., 2007). In this study, the long-established 2D
 323 model known as Finite Element Surface Water Modeling System 3.1.5 (FESWMS) was used to
 324 simulate hydraulics and predict anadromous fish habitat quality and sediment transport regime.
 325 FESWMS solves the vertically integrated conservation of momentum and mass equations using a
 326 finite element method to acquire depth-averaged 2D velocity vectors and water depths at each
 327 node in a finite element mesh. The model is capable of simulating both steady and unsteady 2D
 328 flow as well as subcritical and supercritical flows. The basic governing equations for vertically
 329 integrated momentum in the x - and y - directions under the hydrostatic assumption are given by

$$330 \quad \frac{\partial}{\partial t}(HU) + \frac{\partial}{\partial x}(\beta_{uu}HUU) + \frac{\partial}{\partial y}(\beta_{uv}HUV) + gH \frac{\partial z_b}{\partial x} + \frac{1}{2}g \frac{\partial H^2}{\partial x} \quad (6a)$$

$$+ \frac{1}{\rho_w} [\tau_x^b - \frac{\partial}{\partial x}(H\tau_{xx}) - \frac{\partial}{\partial y}(H\tau_{xy})] = 0$$

331 and

$$332 \quad \frac{\partial}{\partial t}(HV) + \frac{\partial}{\partial x}(\beta_{vu}HVU) + \frac{\partial}{\partial y}(\beta_{vv}HVV) + gH \frac{\partial z_b}{\partial y} + \frac{1}{2}g \frac{\partial H^2}{\partial y} \quad (6b)$$

$$+ \frac{1}{\rho_w} [\tau_y^b - \frac{\partial}{\partial x}(H\tau_{yx}) - \frac{\partial}{\partial y}(H\tau_{yy})] = 0$$

333 where H is water depth; U and V are depth-averaged velocity components in the horizontal x -
 334 and y - directions; z_b is the bed elevation, ρ_w is water density, β_{uu} , β_{uv} , β_{vu} , and β_{vv} are the
 335 momentum correction coefficients that account for the variation of velocity in the vertical
 336 direction; τ_x^b and τ_y^b are the bottom shear stresses acting in the x - and y -directions, respectively;
 337 and τ_{xx} , τ_{xy} , τ_{yx} , and τ_{yy} are the shear stresses caused by turbulence. Conservation of mass in two
 338 dimensions is given by

339
$$\frac{\partial H}{\partial t} + \frac{\partial}{\partial x}(HU) + \frac{\partial}{\partial y}(HV) = 0 \quad (7)$$

340 In this study, FESWMS was used for exploratory numerical experimentation to obtain a
341 conceptual understanding of the potential value of flow reregulation in a constrained regulated
342 gravel-bed river. FESWMS was implemented using the Surface Water Modeling System v. 8.1
343 graphical user interface (EMS-I, South Jordan, UT). The boundary conditions required to run
344 FESWMS are the input hydrograph, the exit water surface elevation, and high-resolution channel
345 topography. In addition, model parameters are needed to describe channel roughness and
346 provide turbulence closure. Values for all boundary conditions and parameters were selected to
347 be physically realistic and were not numerically calibrated. As previously stated, the discharges
348 used were steady values of 8.5 m³/s, 13 m³/s, 70.8 m³/s, and 170 m³/s. Corresponding water
349 surface elevations at the end of the reach were directly observed with a Topcon 802A total
350 station, except for the value associated with 70.8 m³/s, which was obtained using a stage-
351 discharge rating curve.

352 DEM {x,y,z} contour and grid points were imported from AutoCAD into SMS where
353 they were used to interpolate the elevations of the nodes in a finite element mesh consisting of
354 triangular and quadrangular elements. A unique mesh was generated for each discharge to
355 maintain a similar number of computational nodes (~43,000) given that the inundated area
356 increased with discharge and to enable increased resolution of key features relevant to each flow
357 (e.g. steep banks, boulder clusters, riffle crests, and recirculating eddies). Internodal spacing
358 ranged from 0.2-1.0 m for each mesh. To reduce model instability associated with mesh-element
359 wetting and drying at a threshold of 9-cm depth (~D₉₀), meshes were iteratively trimmed to
360 exclude dry areas.

361 The effect of channel roughness on flow was addressed two ways in the model.
362 Roughness associated with resolved bedform topography (e.g. rock riffles, boulders, gravel bars,
363 etc) was explicitly represented in the detailed channel DEM. 2D model predictions are highly
364 sensitive to DEM inaccuracies (Bates et al., 1997; Hardy et al., 1999; Lane et al., 1999; Horritt et
365 al., 2006), which is why such a highly detailed topographic mapping campaign was done in this
366 study. For unresolved roughness, a global Manning's coefficient of 0.043 was used with all
367 meshes based on previous work in similar conditions (Pasternack et al., 2004, 2006; Elkins et al.,
368 2007). This value was not obtained by numerical calibration. It was carefully checked in the
369 validation effort by comparing observed and predicted water surface elevations along the reach
370 at the different discharges as well as by comparing observed and predicted depths and velocities
371 at cross-sections. Although it is possible to vary the bed-roughness parameter spatially in a 2D
372 model to try to account for variable bed sediment facies, it is difficult to justify small (<0.005)
373 local deviations relative to 2D-model and measurement accuracy in gravel bed rivers. 2D
374 models have been reported to be sensitive to large (>0.01) variations in n values (Bates et al.,
375 1998; Lane and Richards, 1998; Nicholas and Mitchell, 2003), and the validation approach used
376 here would reveal that scale of deficiency.

377 In a study of 2D model sensitivity for a bedrock channel, Miller and Cluer (1998) showed
378 that 2D models are particularly sensitive to the eddy viscosity parameterization used to cope with
379 turbulence. In the model used in this study, eddy viscosity (E) was a variable in the system of
380 model equations, and it was computed as

$$381 \quad E = c_0 + 0.6 \cdot H \cdot u^* \quad (8)$$

382 where u^* is shear velocity and c_0 is a minimized constant added for numerical stability (Fischer
383 et al., 1979). This equation was implemented in FESWMS to allow eddy viscosity to vary

384 throughout the channel, which yields more accurate transverse velocity gradients. However, a
385 comparison of 2D and 3D models for a shallow gravel-bed river demonstrated that even with this
386 spatial variation, it is not enough to yield as rapid lateral variations in velocity as occurs in
387 natural channels, presenting a fundamental limitation of 2D models like FESWMS
388 (MacWilliams et al., 2006).

389

390 ***3.4.1. 2D model validation***

391 Recognizing that 2D models, like all models, have inherent strengths and weaknesses,
392 some amount of uncertainty in model results must be understood and accepted (Van Asselt and
393 Rotmans, 2002). Past studies using FESWMS for similar shallow gravel-bed rivers like the
394 Trinity River have validated the model for this application and provide a basis for appreciating
395 model utility and uncertainty (Pasternack et al., 2004, 2006; Wheaton et al., 2004b; MacWilliams
396 et al., 2006; Elkins et al., 2007). In addition to that past work on similar rivers, a new analysis of
397 model uncertainty was done for the LHR on the Trinity River. Since the model parameters were
398 set to physically realistic values and not numerically calibrated to match observations,
399 comparisons of predicted and observed conditions provide a meaningful assessment of model
400 uncertainty.

401 Three different types of validation testing were done to evaluate model performance.
402 First, to validate model performance with regard to the key model parameter of eddy viscosity,
403 the range of E values in model output was checked against field-based estimates at 8.5 m³/s
404 calculated using Eq. (8) with observed depth and velocity measurements at the study's cross-
405 sections. Modeled and measured E values were found to be similar (~0.02-0.1 m²/s).

406 Second, a Topcon total station was used to measure the longitudinal water surface

407 elevation along the reach at 8.5, 13, and 171 m³/s. These profiles were compared against model-
408 produced WSE profiles to test the suitability of the selected Manning's n value of 0.043. The
409 results are reported later for each cross-section at 13 m³/s. For 171 m³/s, modeled WSE was
410 systematically slightly higher than the observed WSE, with the deviation averaging just 5% of
411 mean cross-sectional depth at each observation location (standard deviation of 2.5%). Thus, the
412 prescribed Manning's n value for this highest flow was slightly high, but not enough to warrant
413 iterative calibration.

414 Third, recognizing that lateral and longitudinal variation in velocity in a river is highest at
415 low discharge and low during large floods (Clifford and French, 1998), detailed model validation
416 of depth and velocity on the Trinity River was performed at a low discharge of 13 m³/s using
417 observed depths and velocities from cross sections 1, 2, 3, 13, and 14 (Fig. 5). All cross sections
418 were taken a year after topographic surveying because of time constraints and regulatory flow
419 releases, so the few significant differences in bed topography are attributable to real changes
420 from bed scour, notably at cross section 13. The detailed findings of this aspect of model
421 validation are reported in the results section. Models such as FESWMS are best viewed as
422 uncertain conceptual guides of likely outcomes, rather than literal truth, and that is how it has
423 been used here to yield a balanced array of exploratory numerical modeling and field-based
424 empirical studies to seek the most thorough process-based understanding.

425

426 ***3.4.2. Sediment transport regime model***

427 Shields stress (τ^*) is a variable that characterizes the state of sediment transport in a
428 stream and is defined as

429

430
$$\tau^* = \frac{\tau_0}{(\rho_s - \rho_w)gD_{50}} \quad (9)$$

431
 432 where τ_0 is bed shear stress, ρ_s is sediment grain density, and D_{50} is median grain size (Lisle et
 433 al., 2000). Using the results of the 2D model, τ_0 was first calculated on a nodal basis using
 434 Einstein's log-velocity equation for turbulent flows over rough beds:

435
 436
$$\tau_0 = \rho_w \left(U \left(5.75 \cdot \log \left(\frac{12.2 \cdot H}{4.5 \cdot D_{50}} \right) \right) \right)^2 \quad (10)$$

437
 438 where the value of D_{50} used at each node was the reach-average value. It was infeasible to
 439 measure D_{50} in detail through the reach. The Nikuradse roughness size was taken as $k_s = 4.5 \cdot D_{50}$
 440 after Thompson and Campbell (1979). Equation (10) was then nondimensionalized using Eq. (9)
 441 with the reach-average D_{50} to yield nodal τ^* .

442 The sediment transport regime was characterized by the range of values that τ^* falls into,
 443 as defined by Lisle et al. (2000): values of $0.00 < \tau^* < 0.01$ correspond with no transport; $0.01 <$
 444 $\tau^* < 0.03$ indicates intermittent, localized transport in response to infrequent turbulent bursts
 445 and/or bed vibrations; $0.03 < \tau^* < 0.06$ corresponds with Wilcock et al.'s (1996) domain of
 446 "partial transport" in which grains move in proportion to their relative exposure on the bed
 447 surface; $0.06 < \tau^* < 0.1$ represents full transport of a "carpet" of sediment $1-2 \cdot D_{90}$ thick; and $\tau^* >$
 448 0.1 corresponds with channel-altering conditions. The use of these regime classes helps reduce
 449 the impact of propagation of errors in hydrodynamic prediction, as the classes are much broader
 450 than the precision and accuracy of the predictions (see Pasternack et al., 2006, for evaluation of
 451 such propagation errors and validation of 2D shear stress predictions for shallow gravel-bed

452 rivers). These thresholds are likely to shift down for very loose gravel beds and up for highly
453 compacted and structured gravel beds.

454

455 **3.4.3. *Physical habitat quality model***

456 The physical habitat for coho, chinook, and steelhead spawning, fry, and juvenile life
457 stages as well as the steelhead adult life stage were modeled at 8.5, 13, and 71 m³/s respectively
458 to understand how the anthropogenic boundary controls in the LHR affect the quantity and
459 quality of available habitat as a function of discharge. Fisheries habitat conditions are highly
460 specific to species and life stage (USFWS, 1999; Moyle and Cech, 2003; Hardy and Addley,
461 2001) and are the result of complex chemical, biological, and physical interactions (Stalnaker,
462 1979; Jowett, 1997). Although diverse variables such as temperature, bioenergetics,
463 competition, predation, hyporheic flow, and water quality are known to influence fish behavior,
464 the physical variables of water depth, velocity, and channel-bottom substrate conditions are
465 highly predictive of physical habitat in shallow gravel-bed rivers (Leclerc et al., 1995; Ghanem
466 et al., 1996).

467 By combining the 2D model predictions of depth and velocity with field observations of
468 channel substrates and independently obtained local habitat suitability curves for these three
469 physical variables for each species in each life stage (USFWS, 1999), it was possible to predict
470 the spatial pattern of physical habitat quality (method detailed in Pasternack et al., 2004). The
471 result of this integration was a depth, velocity, and substrate habitat suitability index value
472 (DHSI, VHSI, and SHSI, respectively) at each model node for chinook spawning, fry, and
473 juvenile habitat; steelhead spawning, fry, juvenile and adult habitat; and coho spawning, fry and
474 juvenile habitat. Because nonspawning life stages are much less dependent on substrate quality,

475 a global habitat suitability index (GHSI) was calculated as the geometric mean using $GHSI =$
476 $DHSI^{0.5} \times VHSI^{0.5}$ for those cases, giving depth and velocity equal weighting (e.g. Leclerc et al.,
477 1995; Cavallo et. al., 2003; Elkins et al., 2007). Similarly, GHSI values for spawning habitat
478 were calculated as the geometric mean using $GHSI = DHSI^{0.3} \times VHSI^{0.3} \times SHSI^{0.3}$, giving depth,
479 velocity, and substrate equal weighting (e. g. Gard, 2006). GHSI was calculated on a nodal basis
480 and classed as poor (0-0.1), low (0.1-0.4), medium (0.4-0.7), and high (0.7-1.0) quality habitat
481 adopting the system of Leclerc et al., (1995). This grouping helps account for 2D model and HSI
482 uncertainty by averaging over a range of GHSI values, as there is no ecological basis for
483 distinguishing GHSI at a finer resolution at this time. The effect of flow reregulation on the
484 amount of physical habitat was evaluated by comparing the amount of medium- and high-quality
485 habitat ($GHSI > 0.4$) for all species and life stages for the three modeled discharges. For brevity
486 and illustrative purposes, detailed spatial patterns of habitat quality are presented for chinook
487 only, with results for the other species and life stages summarized in a single figure. Full details
488 for the other species and life stages are available on-line at the address provided in the results
489 section.

490

491 **4. Results**

492 Empirical and numerical results both show that anthropogenic boundary controls in LHR
493 significantly impact hydrogeomorphic processes key to river rehabilitation, including the
494 recovery of physical habitat for anadromous fish. Key metrics from the detailed analyses
495 performed are reported below. Full simulation results are available to the public from the U.S.
496 Bureau of Reclamation or the corresponding author upon request.

497

498 **4.1. Empirical metrics of channel conditions**

499 The cumulative frequency distributions of bed material grain size shows that the bed is
500 very coarse (Fig. 6). The median particle size (D_{50}) of the LHR is 61.1 mm with a standard
501 deviation of 27 mm. Cross sections 2 and 3 are located in the pool after riffle 1; and they have
502 significantly finer bed material, with D_{50} of 32.1 and 38.2 mm, respectively. Cross sections 4
503 and 10 illustrate armoring of artificial riffles, with D_{50} of 120.7 and 72.6 mm, respectively (not
504 counting the large, placed boulders). Along with these geomorphic unit differences in grain size,
505 facies mapping revealed that there are local lateral variations caused by anthropogenic activities.
506 These include finer particle sizes occupying the hatchery outfall scour pools (Fig. 5) as well as
507 16-32 mm gravels on a relic gravel-injection bar near the end of the reach.

508 The distribution of slope within the LHR is directly related to anthropogenic boundary
509 controls. The long profile has an overall slope of 0.0022, with significantly higher slopes
510 occurring over rock-riffles (Fig. 7). Although the thalweg bed profile shows a lot of variability,
511 the water surface profiles for 8.5 and 13 m³/s clearly identify the artificial riffles located at 0,
512 125, 270, and 450 m as slope control structures. The profile begins at riffle 1 and slopes to riffle
513 2 at 0.0017. From riffle 2 to the downstream pool located at a bedrock constriction (Figs. 3,5),
514 the channel slope increases to 0.0298. The slope from riffle 3 to 4 is 0.052. The distribution of
515 slope over the rock-riffles is not distributed evenly. The majority of the slope in the LHR is lost
516 over riffle 2. This slope is associated with the dense cluster of wired, 1.25-m-diameter boulders
517 that help hold the smaller cobbles and boulders comprising the feature.

518 The average hydraulic geometry exponents (b, f, m) for the LHR cross sections are 0.17,
519 0.50, and 0.33, respectively (Table 2). These suggest that depth responds most strongly to
520 changes in discharge. Excluding cross section 14, which is not as confined on the river right, the

521 standard deviation of the width exponent is 0.04, so the variation is 15% of the mean value.
522 Comparing pools and riffles, the average hydraulic geometry exponents for the former are 0.19,
523 0.49, and 0.32, with standard deviations of 0.14, 0.09, and 0.05, while those for the latter are
524 0.16, 0.51, and 0.34 with standard deviations of 0.05, 0.03, and 0.02. The significance of this
525 close similarity is that there is no reversal expected for any of these variables as discharge
526 increases. For example, for discharges ranging from 8.5-285 m³/s, riffles always have a greater
527 velocity and bed shear stress than pools (Fig. 8).

528

529 *4.2. 2D Model predictions*

530 To address the key questions of this study the 2D model results were divided into
531 sections evaluating hydraulics, sediment transport, and physical habitat. For each of these
532 regimes anthropogenic boundary controls were found to have a dominating influence over the
533 spatial distribution of all metrics of hydrogeomorphic and ecological functionality assessed.

534

535 *4.2.1. 2D Model Validation*

536 The primary validation of model-predicted depths and velocities was performed at 13
537 m³/s, which is representative of the July through March low-flow conditions. Lateral patterns of
538 depth predicted by the 2D model at this flow for the five test cross sections closely match those
539 observed, except for cross section 13 that likely experienced scour during the period between
540 topographic surveying and model-validation data collection (Fig. 9). The similarity in predicted
541 and observed depths suggests that the topographic survey and associated DEM were of sufficient
542 resolution to capture bed features. It also demonstrates that the physically realistic bed-
543 roughness parameter (Mannings *n*) used globally was well estimated. In contrast, 2D-model

544 velocity predictions show more scatter relative to observed values, with deviations typically 15-
545 30%. At some points, velocity error is very high. The lateral pattern of velocity magnitude
546 successfully mimics observed conditions, but as is commonly seen with 2D models, smoothing is
547 excessive. This is attributable to inadequate variation in eddy viscosity that cannot be further
548 improved with these models (Pasternack et al., 2006). Using too high of an eddy viscosity value
549 enables greater transference of momentum, hence the smoothing (MacWilliams et al., 2006). A
550 comparison of observed versus model-predicted water surface slopes for 171 m³/s found that the
551 model matched observed conditions very well. Although it would be ideal to have velocity
552 validation for all flows, the pattern of the velocity field is much more uniform at higher flows,
553 and thus the model can be expected to perform better at higher discharges.

554 Model validation of the LHR on the Trinity River once again revealed the strengths and
555 limitations of 2D modeling of shallow gravel-bed rivers along lines previously reported (Lane et
556 al., 1999; Pasternack et al., 2004, 2006; Wheaton et al., 2004b; MacWilliams et al., 2006; Elkins
557 et al., 2007). The 2D model is accurate enough to provide confidence that the reported spatial
558 patterns in depth and velocity are real, but is not accurate enough to precisely characterize
559 regions with very strong lateral variation, for which 3D numerical modeling would be necessary.
560 In the spirit of scientific exploration, we think the value of 2D modeling in this study outweighs
561 the inherent uncertainty associated with modeling.

562

563 4.2.2. *Hydraulic spatial patterns*

564 The distribution of depth and velocity in the LHR is controlled by anthropogenic
565 boundary controls regardless of discharge. From 8.5 m³/s to 170 m³/s, hydraulic conditions
566 become more uniform, as the spatial patterns of depth and velocity become less influenced by

567 local topography and the artificial riffles, and are governed to a great degree by the channel
568 banks. At $8.5 \text{ m}^3/\text{s}$, local topography controls the distribution of depth and velocity and is
569 disrupted at the four artificial riffles (Figs 10A, 11A). Each riffle creates an area of peak
570 velocities and non-uniform flow patterns. Immediately downstream of each riffle eddies and
571 complex flow patterns are present. Between riffles velocity vectors follow local topography,
572 with the bedrock outcropping between riffles 2 and 3 and the gravel injection bar having the
573 greatest affect on flow direction. At $13 \text{ m}^3/\text{s}$, hydraulic conditions change very little, except that
574 riffles 3 and 4 have velocity and depth patterns that deviate less from the surrounding upstream
575 and downstream areas between riffles (Figs. 10B, 11B). At $71 \text{ m}^3/\text{s}$ the channel boundaries
576 become more uniform and the valley walls on the river right and the hatchery walls on the river
577 left govern the velocity vectors. (Figs. 10C, 11C). Velocity and depth are comparatively more
578 uniform than lower discharges from riffle 1 to 2. The bedrock constriction after riffle two
579 provides the only area of flow convergence in the channel. Flow direction and magnitude vary
580 little after the bedrock constriction to the end of the model despite differences in depth from local
581 topography. The highest peak flow release from the Lewiston Dam during the study was 170
582 m^3/s . Velocity vectors were omitted for clarity and follow a similar distribution to $71 \text{ m}^3/\text{s}$ (Fig.
583 11C), being almost perfectly parallel to the channel banks. Peak velocity zones in the channel
584 did not migrate upstream or downstream, but became more uniform with discharge. There was
585 not a velocity reversal in the channel at $170 \text{ m}^3/\text{s}$ (Fig. 11).

586

587 *4.2.3. Depth-velocity joint distribution*

588 The combination of depth and velocity values in a fluvial geomorphic unit has long been
589 used as an indicator of the meso-scale habitat present (Coarer, 2007). Stewardson and McMahon

590 (2002) showed that depth and depth-averaged velocity are codependent variables, because
591 channel hydraulics exhibit spatial organization. Besides showing how to obtain independent
592 variables, they also used the joint probability distribution of the two codependent variables to
593 show that it is possible to distinguish between two types of channels (i.e. two hydraulic
594 signatures)- one in which velocity and depth are inversely related and one in which they are
595 directly related. The former relation occurs when the channel has a much stronger longitudinal
596 variation in depth than a lateral variation, and vice versa for the latter relation. Whereas
597 Stewardson and McMahon (2002) focus on how these hydraulic signatures can be explained by
598 different channel morphologies, the results of this study demonstrate that the same channel
599 morphology can shift its hydraulic signature as discharge increases (Fig. 12). This effect of
600 decreasing relative roughness and increasing prismatic channel conditions on hydraulic signature
601 as discharge increases is known (e.g. Clifford and French, 1998), but its significance for
602 geomorphic and ecological applications has not been sufficiently explored.

603 The effects of artificial riffles and channel confinement imposed by the hatchery terrace
604 on hydraulic behavior in the LHR are evident in the shifting pattern of the joint distribution of
605 local depth and local velocity as a function of discharge (Figs. 12B,C). For discharges $< 13 \text{ m}^3/\text{s}$,
606 velocity decreases as depth increases. At these discharges, the hydraulic regime is characterized
607 by a wide range of velocities (0-5 m/s) when depth is $< 0.5 \text{ m}$ and a narrow range of low
608 velocities when depth $> 0.5 \text{ m}$. For these discharges, local velocity is controlled by local
609 topographic perturbations that yield pronounced local convective accelerations. Over the
610 artificial riffles, flow is supercritical, so shallow depths have very high velocities; while along
611 rough channel margins, velocities are stagnant. At $71 \text{ m}^3/\text{s}$, small local topographic perturbations
612 associated with depths $< 0.5 \text{ m}$ no longer controlled the hydraulic regime (Fig. 12C). At 170

613 m^3/s , valley confinement by the hatchery terrace yields an essentially prismatic channel with a
614 parabolic lateral velocity distribution, thereby yielding the highest velocities in the deepest part
615 of the channel (Fig. 12D). Two hydraulic regimes are evident in the channel from these
616 analyses. The first regime is a decreasing velocity with increasing depth associated with
617 convective accelerations over and around larger bed perturbations, such as the artificial “rock-
618 weir” riffles, large individual boulders, and boulder clusters submerged to a depth of 0.5-1.25 m.
619 The less submerged these features are, the more the flow approaches and exceeds the critical
620 threshold. The second regime, which occurred at and above $71 \text{ m}^3/\text{s}$ is the valley confinement
621 hydraulic regime in which velocity increases as depth increases, indicating uniform flow
622 conditions.

623

624 4.2.4. *Sediment transport*

625 Boundary controls were observed to influence the distribution of Shields stress in the
626 LHR. Regardless of discharge, Shields stress peaks over the rock riffles in bands perpendicular
627 to the channel edge (Fig. 13). At successively higher discharges, confinement causes
628 longitudinal growth of areas of mobility. At $8.5 \text{ m}^3/\text{s}$, 90% of the channel is predicted to
629 experience no transport, while 6% of the channel is expected to experience selective transport,
630 2% experiences partial transport, and 2% experiences full transport conditions (Fig. 14). Riffles
631 1 and 2 have exhibit areas of full mobility associated with the tops of boulders in the riffles. Past
632 riffle 2 at the bedrock constriction, an area of selective transport is evident. Riffles 3 and 4 are
633 predicted to experience select transport. At $13 \text{ m}^3/\text{s}$, patterns of selective transport at the rock
634 riffles and bedrock constriction expand in the downstream direction. Three distinct shear zones
635 are also evident over three boulders past riffle 1 on the river right that have adjacent selective

636 transport patches on the left. Riffle 2 shows two bands of selective transport extending
637 downstream ~ 40 m from the riffle crest. Selective transport is predicted over 11% of the
638 channel, while 2% of the channel is predicted to experience partial transport, and 2% experiences
639 full transport conditions. Areas of selective transport increase to 74% of the channel and extend
640 from rock riffle to rock riffle at 71 m³/s (Fig. 14). Partial transport is limited to 11% of the
641 channel over the rock riffles, the bedrock constriction, and in several lateral bands between
642 riffles 1 and 2. At 170 m³/s, 64% of the channel is in at least partial transport in a longitudinal
643 band in the center of the channel that begins at riffle 1 and extends downstream. The channel
644 edges experience selective transport at this discharge.

645

646 4.2.5. *Physical habitat*

647 For brevity, detailed illustration of the spatial distribution of physical habitat is limited to
648 only one species in one life stage (Fig. 15) with the analyses of all others summarized in Fig.14.
649 All detailed habitat-quality maps for the Trinity River may be viewed at
650 <http://shira.lawr.ucdavis.edu>. The spatial pattern of fall-run chinook spawning habitat quality
651 was predicted with and without consideration of substrate quality. When substrate is not
652 considered, spawning habitat is predicted to be very abundant in the LHR with 77% being at
653 least medium quality at 8.5 m³/s (Fig. 16A). However, when the SHSI is utilized the 2D model
654 predicted chinook spawning habitat decreases to 36% of the total area (Fig. 16b). The reason for
655 this is that the bed is heavily armored, with just a few locations with the desirable size range of
656 gravels and cobbles. Regardless of whether or not an SHSI was utilized, little to no chinook
657 spawning habitat was predicted within 15 m of the artificial riffles, indicating that these
658 structures are heavily armored and flow over them is too fast.

659 The spatial distribution of chinook juvenile and fry rearing habitat are controlled by
660 lateral bars, artificial riffles, and historical gravel injection sites (Figs. 15C,D). Chinook fry
661 prefer very shallow and slow-moving channel margins. The majority of the channel is predicted
662 to be either low or very poor quality rearing habitat for chinook fry, as the channel is relatively
663 prismatic. However, the 2D model turns off any element with < 9 cm depth, because that is
664 close to D_{90} and causes model instability. Thus, the model may be under representing the
665 available fry habitat for a thin strip of sheet flow along each bank. This represents an important
666 limitation for the use of 2D models in habitat evaluation.

667 Chinook juvenile rearing habitat follows a similar spatial distribution as that of chinook
668 fry, but with a shift in habitat preference to deeper areas with low velocities. The central third of
669 the channel is predicted to range from low to medium quality because the velocity is too high.
670 High quality habitat is present on lateral bars, including remnant gravel deposits at historical
671 gravel injection sites, with the largest being on river left at the end of the reach.

672 Steelhead, chinook, and coho spawning and fry habitat quality spatial patterns at $8.5 \text{ m}^3/\text{s}$
673 are relatively similar in reflecting hydrodynamics, but with different percentages of habitat
674 quality classes (Fig. 16). Coho and steelhead spawning habitat are both more abundant than
675 chinook spawning habitat. In contrast, the limited amount of chinook juvenile rearing habitat,
676 for steelhead is much more ubiquitous throughout the reach, along with steelhead adult holding
677 habitat, because steelhead juveniles (and adults) prefer 1-3 times higher velocities than chinook
678 juveniles. Whereas steelhead juveniles prefer higher velocities than chinook juveniles, coho
679 juveniles prefer significantly lower velocities, and thus their rearing habitat availability in the
680 reach is greatly reduced. Thus, during fall and winter low flows, this upstream-most reach has a
681 reasonable abundance of steelhead and chinook juvenile rearing and adult holding habitat, but a

682 significant lack of steelhead and chinook spawning habitat. Availability of all coho life stage
683 habitats is inadequate, but that species is not primarily managed for in this reach

684 A central aim of this study is to quantify the response of physical habitat quantity to
685 changes in discharge, which is a very important component of evaluating the potential
686 effectiveness of flow reregulation on fisheries restoration. A near doubling of the low-flow
687 release is predicted to cause dramatic decreases in the percent of medium and high quality
688 physical habitat for most species' life stages within the LHR (Fig. 16). The change from 8.5 to
689 13 m³/s substantially reduces the percent of at least medium quality of the physical habitat for all
690 three species' life stages except chinook and steelhead juvenile habitat, steelhead adult habitat,
691 and chinook and coho fry habitat, with these last two already near zero. Only 0-3% of the
692 channel is predicted to be at least medium quality fry habitat at 8.5 m³/s, and this increases by
693 3% for chinook fry and 1% for coho fry at 13 m³/s. Medium plus high quality habitat for
694 steelhead adult and juveniles increases by 3 and 1%, respectively; while chinook juvenile habitat
695 of this quality decreases by 13% from 8.5 to 13 m³/s. Spawning habitat for steelhead, chinook,
696 and coho decreases by 37, 22, and 43%, respectively, from 8.5 to 13 m³/s.

697 When flow is increased from 13 to 71 m³/s the percent of the channel that is at least
698 medium quality habitat decreases sharply for all species' life stages to below 5% of channel area,
699 except steelhead adult habitat (Fig. 16), which still was present in medium or high quality over
700 27% of the channel. Medium and high quality coho fry rearing habitat showed an insignificant
701 increase in habitat area with this change, but remained below 5%. Further flow increases
702 assessed for Shields stresses were not evaluated for habitat quality, as the channel was too deep
703 and fast to have any significant fish habitat.

704

705 **5. Discussion**

706

707 *5.1. Effect of anthropogenic valley confinement*

708 Anthropogenic valley confinement in the LHR through construction of the Lewiston
709 Hatchery has had the commonly observed effect on geomorphology, hydraulics, and fisheries for
710 alluvial rivers (Bowen et al., 2003; Jacobson and Galat, 2006). Variations in channel width has
711 in many ways been linked to hydraulic conditions that contribute to geomorphic and ecological
712 variability (Coulombe-Pontbriand and Lapointe, 2004). In reaches where channel width is
713 constant, such as the study reach, hydraulic conditions are promoted that lead to monotony in
714 geomorphic form and in resultant ecological habitat. In this study, empirical and numerical tests
715 for the study reach both came to the same conclusion that a confined and restricted width affects
716 existing and potential fisheries restoration. The lack of variation in channel width between riffle
717 and pool sections, coupled with the cross section averaged velocity being always faster over
718 riffles than pools, limits the potential for geomorphic sustainability in the LHR, as no hydraulic
719 reversals in mean conditions were empirically detected. Hydraulic geometry analysis results are
720 reinforced by 2D model results for depth, velocity, and their joint distribution. For flows < 13
721 m³/s, local topographic features control the distribution of depth and velocity between riffles, and
722 channel width displays moderate control on flow vectors. However, at 71 m³/s channel width
723 becomes very uniform and 2D model results show that hydraulic variables display less
724 variability and uniform, subcritical flow conditions dominate. The 2D model did not detect any
725 velocity reversals for the reach. The distribution of Shields stress is controlled by local
726 topography and the riffles below 13 m³/s. Increases in discharge cause the distribution of Shields
727 stress to grow from transverse bands associated with the artificial riffles to longitudinal tubes

728 down the central third of the channel, especially at $170 \text{ m}^3/\text{s}$. Such a distribution of Shields
729 stress shows that the channel banks exhibit a fundamental control on sediment transport and bed
730 morphology in the study reach. The lateral bars between riffles provide the majority of the
731 physical habitat for all lifestages in the LHR, but have unsuitable depths at $71 \text{ m}^3/\text{s}$. The net
732 effect of valley confinement on physical habitat in the LHR is that shallow water habitat is
733 nonexistent for flows $>71 \text{ m}^3/\text{s}$.

734

735 *5.2. Effect of artificial riffles*

736 Artificial riffles fix the bed slope of the LHR and create local zones of high bed slope,
737 velocity, and Shields stress. The riffle-pool units in the LHR do not appear to be sustainable, as
738 log-log plots of velocity versus depth for riffle-pool sections as well as 2D model results for
739 velocity and Shields stress indicate that riffles are always faster than pools. These results do not
740 account for forced pools associated with vortex shedding and convective acceleration, but flow
741 reregulation would not induce such forced pools anyway. The artificial riffles are also predicted
742 to experience a “full transport” sediment-transport regime with regards to the median particle
743 size of the reach at all discharges modeled. This instability is verified as riffles 1, 2, and 3 that
744 are heavily armored, implying that smaller gravels have a low probability of occurrence from
745 hydraulic forces. Gravel instability at artificial riffles during flow $< 13 \text{ m}^3/\text{s}$ has led to infilling
746 of downstream pools, decreasing bed relief and forming monotonous runs. Median particle sizes
747 on some parts of the riffles are adequate for Chinook spawning, but velocities are still too high.
748 Thus, most spawning is predicted and has been independently observed by the authors to occur
749 on lateral bars in the study area between the riffles. Also, Elkins et al. (2007) experimentally
750 created a chute with lateral bars in a different regulated gravel bed river and observed that the

751 fish shifted their spawning pattern to line up on those bars adjacent to the high-velocity chute.
752 These peripheral locations may have poor hyporheic water quality and low embryo survival to
753 the fry life stage.

754

755 *5.3. The potential for salmonid habitat restoration in the LHR by flow reregulation*

756 Existing physical habitat in the reach is of relatively poor quality and diminishes quickly
757 as flow increases. Spawning habitat is not associated with riffles, but rather with lateral bars
758 between the rock riffles. Potentially these areas experience little upwelling and hyporheic flows
759 possibly affecting embryo mortality rates. Riffle velocities are too fast and substrate too coarse
760 for spawning.

761 River rehabilitation for salmonids requires that suitable habitat be available for all
762 lifestages. At the spawning discharge of $8.5 \text{ m}^3/\text{s}$, the amount of available medium and high
763 quality spawning habitat as a percentage of the total area is 36% for chinook, 50% for coho, and
764 44% for steelhead, including significant overlap on the same lateral bar morphologic units.
765 These values drop significantly for even a modest flow increase to $13 \text{ m}^3/\text{s}$ and are virtually
766 nonexistent by $71 \text{ m}^3/\text{s}$. These decreases are linked to the hydraulic response of the channel from
767 unnatural confinement and from the focusing of energy dissipation at oversteepened rock riffles,
768 whereby increases in discharge concentrate velocity and Shields stress on riffles at low flows and
769 in the central thalweg at high flows.

770 In contrast to the current condition in which flow reregulation would not improve
771 salmonid habitat, the historical channel configuration (Fig. 2) lacked confinement and bed steps.
772 An increase in discharge under historical morphological conditions would have activated
773 secondary and tertiary channels across a wide active gravel valley bottom, creating more areas of

774 shallow water with low to moderate velocities that match the conditions desired for fish
775 spawning and rearing identified by USFWS (1999). That would provide ample physical habitat
776 at all flows up to the threshold for filling the valley completely. Jacobson and Galat (2006)
777 performed a numerical experiment comparing historical and modern shallow water habitat for a
778 similarly confined river and reported this type of outcome. Thus, the benefits of a natural flow
779 regime are dependent on the presence of a wide and connected channel-floodplain system.

780 In determining adequate flows for instream fisheries needs, many have relied on
781 statistical methods that relate fish escapement to frequency of flow occurrence (Jowett, 1997;
782 Maddock, 1999). This approach yields the recommendation of instituting a “scaled down”
783 hydrograph in which the natural timing and duration of discharge fluctuations are mimicked with
784 flow releases by the dam, but at a reduced flow magnitude. However, little or no consideration
785 has been given of geometric constraints that control flow and sediment transport responses to
786 discharge at the hydraulic and geomorphic unit scales. Channel geometry varies significantly
787 along alluvial rivers depending on the local balance of transport capacity versus sediment supply
788 (Leopold et al., 1964; Lisle et al., 2000). This study adds to a growing body of work (Bowen et
789 al., 2003; Jacobson and Galat, 2006) that suggests that consideration of channel geometry, and
790 subsequent controls on its adjustment, need be considered along with flow reregulation as human
791 and biological activities during interim flow regulation can impact channel geometry and thus
792 hydraulic and geomorphic processes that drive physical habitat.

793 While past studies detail constraints on sediment transport and physical habitat in
794 regulated reaches (Bowen et al., 2003; Jacobson and Galat, 2006), few explicitly define causal
795 mechanisms associated with geomorphic processes at the hydraulic unit and geomorphic unit
796 scales with implications to flow-based restoration strategies. Two fundamental processes will

797 likely govern bed-morphology evolution and thus the abundance of physical habitat in the LHR.
798 At flows $< 13 \text{ m}^3/\text{s}$, an unarmored bed will be unstable at step-like riffle units. Any loose
799 particles available for transport will be hydraulically sorted between riffles. At flows $> 170 \text{ m}^3/\text{s}$,
800 the partial transport over riffles gives way to a continuous thalweg experiencing partial transport.
801 The presence of lateral gravel bars is morphological evidence that this pattern of thalweg scour is
802 occurring in the LHR. The implication is that natural development of riffle-pool differentiation
803 and habitat heterogeneity is inhibited at low flow by the artificial riffles and at high flow by
804 anthropogenic valley confinement. As physical habitat in alluvial rivers is considered to be
805 heavily dependent on spatially nested morphologic features, anthropogenic boundary controls
806 that limit or prohibit bedform development can ultimately serve as a limiting factor in salmonid
807 habitat restoration.

808

809 **6. Conclusion**

810 In this study, we found that anthropogenic boundary controls in the LHR have disrupted
811 the natural linkages between hydrologic, geomorphic, and ecological processes independently of
812 the changes in the natural flow regime associated with flow regulation. Rock riffles controlling
813 energy slope at discharges $< 71 \text{ m}^3/\text{s}$ have fixed channel morphology and hydraulics, preventing
814 any dynamic equilibrium between flow, sediment, and hydraulic geometry. Moreover, riffle exit
815 slopes create areas of high shear stress that prohibit both stability of spawning-sized gravels and
816 spawning activity. The fish hatchery adjacent to the straight channel acts as a lateral boundary
817 control prohibiting any channel migration and overbank dynamics, prohibiting self-development
818 of riffle-pool units under the commonly understood mechanisms for their formation and self-
819 maintenance. Because of vertical and lateral boundary controls, we concluded that reregulation

820 of flow would do little for improving salmonid habitat in the LHR where large numbers of
821 anadromous fish come to spawn.

822 Beyond serving as a specific example of conditions on a local reach on a regulated
823 gravel-bed river, this study illustrates how geomorphic and 2D hydrodynamic tools may be
824 integrated to identify specific mechanisms underlying complex river management problems.
825 Also, it shows that for sediment starved reaches experiencing confinement that a distinct pattern
826 of velocity, depth, and shear stress will develop with implications to the distribution of physical
827 habitat of salmonids. Substrate suitability should be accounted for in heavily armored sites to
828 more accurately predict physical habitat. Moreover, it shows that from an evaluation perspective
829 artificial riffles that function as rock-weirs to limit channel incision can prohibit morphologic
830 adjustment and create hydraulic conditions unsuitable for fisheries use.

831

832 **7. Acknowledgements**

833 Financial support for this work was provided by USBR Award #03FG230766 through the
834 Trinity River Restoration Program and USFWS Agreement DCN#113322G003 awarded by
835 CALFED. We gratefully thank and acknowledge Eve Elkins, Marisa Escobar, Dr. Peng Gao, Dr.
836 Mark Grismer, Dr. Joe Merz, Dr. Hamish Moir, Dr. Jeff Mount, and Joe Wheaton for their input
837 on this manuscript. We thank Michael Bounrisavong and Kaushal Parikh for their help
838 performing 2D model simulations. We thank Carlos Alvarado, Andy Tranmer, and Evan
839 Buckland for field support. We thank anonymous reviewers, David Montgomery, and editor
840 Dick Marston for detailed and constructive input that improved the quality of the article.

841

842 **8. References**

843

844 Abbe, T.B., Montgomery, D. R.; 1996. Large woody debris jams, channel hydraulics, and habitat
845 formation in large rivers. *Regulated Rivers: Research & Management* 12, 201-222.

846 Abbe, T., Pess, G., Montgomery, D. R., and Fetherston, K., 2003. Integrating engineered log jam
847 technology into reach-scale river restoration, in Montgomery, D. R., Bolton, S., Booth, D. B.,
848 and Wall, L., (editors) *Restoration of Puget Sound Rivers*, University of Washington Press,
849 Seattle and London, pp. 443-482.

850 Babakaiff, S., Hay, D., Fromouth, C., 1997. Rehabilitating stream banks. In: Slaney, P.A.,
851 Zaldokas, D. (Eds.), *Fish Rehabilitation Procedures*. British Columbia Ministry of
852 Environment, Lands and Parks, *Watershed Restoration Technical Circular No. 9*, Vancouver,
853 B.C.

854 Bates, P.D., Anderson, M.G., Baird, L., Walling, D.E., Simm, D. 1992. Modelling floodplain
855 flow with a two dimensional finite element scheme. *Earth Surface Processes and Landforms*
856 17, 575-588.

857 Bates, P.D., Anderson, M.G., Hervouet, J. M., Hawkes, J.C., 1997. Investigating the behaviour
858 of two-dimensional finite element models of compound channel flow. *Earth Surface*
859 *Processes and Landforms*, 22(1), 3-17.

860 Bates, P.D., Horritt, M. S., Hervouet, J.M., 1998. Investigating two-dimensional, finite element
861 predictions of floodplain inundation using fractal generated topography. *Hydrological*
862 *Processes*, 12(8), 1257-1277.

863 Booker, D.J., Sear, D.A., Payne, A.J., 2001. Modeling three-dimensional flow structures and
864 patterns of boundary shear stress in a natural pool-riffle sequence. *Earth Surface Processes*
865 *and Landforms* 26(5), 553-576.

866 Bosch, J.M., Hewlett, J.D., 1982. A Review of Catchment Experiments to Determine the Effect
867 of Vegetation Changes on Water Yield and Evapo-Transpiration. *Journal of Hydrology* 55(1-
868 4), 3-23.

869 Bowen, Z.H., Bovee, K.D., Waddle, T.J.; 2003. Effects of Channel Modification on Fish Habitat
870 in the Upper Yellowstone River; U.S. Geological Survey Open-File Report 03-476,
871 Washington, D.C.

872 Buffington, J.M., Lisle, T.E., Woodsmith, R.D., Hilton, S. 2002; Controls on the size and
873 occurrence of pools in coarse-grained forest rivers. *River Research and Applications*.18, 507-
874 531.

875 Cao, Z., Carling, P., Oakey, R., 2003. Flow reversal over a natural pool-riffle sequence: a
876 computational study. *Earth Surface Processes and Landforms* 28, 689-705.

877 Carling, P.A., 1991. An appraisal of the velocity-reversal hypothesis for stable pool-riffle
878 sequences in the River Severn, England. *Earth Surface Processes and Landforms* 16, 19-31.

879 Cavallo, B., Kurth, R., Kindopp, J., Seesholtz, A., Perrone, M., 2003. Distribution and habitat
880 use of steelhead and other fishes in the lower feather river, 1999-2001. Interim Report.
881 SPF10, Task 3a, California Department of Water Resources, Division of Environmental
882 Services.

883 Cederholm, J.C., Dominguez, L.G., Bumstead, T.W., 1997. Rehabilitating stream channels and
884 fish habitat using large woody debris. In: Slaney, P.A., Zaldokas, D. (Eds.), *Fish*
885 *Rehabilitation Procedures*. British Columbia Ministry of Environment, Lands and Parks,
886 Watershed Restoration Technical Circular No. 9, Vancouver, B.C.

887 Chang, H. H. 1988. *Fluvial Processes in River Engineering*. John Wiley and Sons, New York.

888 Clifford, N. J., French, J. R., 1998. Restoration of channel physical environment in smaller,
889 moderate gradient rivers: geomorphological bases for design criteria. In: Bailey, R. G., Jose,
890 P. V., Sherwood, B. R. (Eds.), United Kingdom Floodplains. Westbury Academic &
891 Scientific Publishing, Westbury, pp. 72-76.

892 Clifford, N.J., Richards, K., 1992. 2: The reversal hypothesis and the maintenance of riffle-pool
893 sequences: a review and field appraisal. In: Carling, P., Petts, G. (Eds.), Lowland Floodplain
894 Rivers: Geomorphological Perspectives. John Wiley and Sons Ltd, Chichester, UK, pp. 43-
895 70.

896 Coarer, Y.L., 2007. Hydraulic signatures for ecological modelling at different scales. *Aquatic*
897 *Ecology*: DOI 10.1007/s10452-005-9005-3.

898 Constantine, C.R., Mount, J.F., Florsheim, J.L., 2003. The Effects of Longitudinal Differences in
899 Gravel Mobility on the Downstream Fining Pattern in the Cosumnes River, California.
900 *Journal of Geology* 111, 233-241.

901 Constantine, J.A., Pasternack, G.B., Johnson, M.L., 2005. Logging effects on sediment flux
902 observed in a pollen-based record of overbank deposition. *Earth Surface Processes and*
903 *Landforms* 30, 813-821.

904 Coulombe-Pontbriand, M. and Lapointe, M., 2004. Geomorphic controls, riffle substrate quality,
905 and spawning site selection in two semi-alluvial salmon rivers in the Gaspé Peninsula,
906 Canada. *River Research and Applications* 20(5), 557-590.

907 Elkins, E.E., Pasternack, G.B., Merz, J.E., 2007. The use of slope creation for rehabilitating
908 incised, regulated, gravel-bed rivers. *Water Resources Research* 43, W05432,
909 doi:10.1029/2006WR005159.

910 Erskine, W. D., 1992. Channel response to large-scale river training works- Hunter River,
911 Australia. *Regulated Rivers- Research and Management* 7(3), 261-278.

912 Fischer, H.B., List, E.J., Koh, R.C.Y., Imberger, J., Brooks, N.H., 1979. *Mixing in Inland and*
913 *Coastal Waters*. Academic Press, Inc., New York, 483 pp.

914 French J.R., Clifford N.J., 2000. Hydrodynamic modeling as a basis for explaining estuarine
915 environmental dynamics: Some computational and methodological issues. *Hydrological*
916 *Processes* 14, 2089-2108.

917 Galat, D. L., Lipkin, R., 2000. Restoring ecological integrity of great rivers: historical
918 hydrographs aid in defining reference conditions for the Missouri River. *Hydrobiologia* 442,
919 29-48.

920 Gard, M. 2006., Modeling changes in salmon spawning and rearing habitat associated with river
921 channel restoration. *International Journal of River Basin Management* 4(2), 1-11.

922 Ghanem A., Steffler, P., Hicks, F., 1996. Two-dimensional hydraulic simulation of physical
923 habitat conditions in flowing streams. *Regulated Rivers: Research & Management* 12, 185-
924 200.

925 Graf, W.L., 1996. Geomorphology and policy for restoration of impounded american rivers:
926 What is 'Natural'? In: Rhoads, B. L., Thorn, C. E. (Eds.), *The Scientific Nature of*
927 *Geomorphology*. Proceedings of the 27th Binghamton Symposium in Geomorphology held
928 September 27-29. John Wiley and Sons, New York.

929 Grant, G.E., Schmidt, J.C., Lewis, S.L., 2003. A geological framework for interpreting
930 downstream effects of dams on rivers. In: O'Connor, J. E., Grant, G. E. (Eds.), *A Peculiar*
931 *River*. American Geophysical Union, Water Science and Application Series #7 Washington,
932 D. C., 209-225.

933 Gray, D.H., Leiser, A.T., 1982. Biotechnical Slope Protection and Erosion Control. Van
934 Nostrand Reinhold Company, New York.

935 Hardy, T.B., Addley, R.C. 2001. Evaluation of Interim Instream Flow Needs in the Klamath
936 River, Phase II Final Report. Institute for Natural Systems Engineering, Utah State
937 University, Logan.

938 Hardy, R.J., Bates, P.D., Anderson, M.G., 1999. The importance of spatial resolution in
939 hydraulic models for floodplain environments. *Journal of Hydrology*, 216(1-2), 124-136.

940 Horritt, M.S., Bates, P.D., Mattinson, M.J., 2006. Effects of mesh resolution and topographic
941 representation in 2D finite volume models of shallow water fluvial flow. *Journal of*
942 *Hydrology*, 329(1-2), 306-314.

943 Hunter, C.J. 1991. Better Trout Habitat: A Guide to Stream Restoration and Management.
944 Island Press, Washington, D.C.

945 Jacobson, R.B., 1995. Spatial controls on patterns of land-use induced stream disturbance at the
946 drainage-basin scale-- An example from gravel-bed stream of the Ozark Plateaus, Missouri.
947 In: J.E. Costa, A.J. Miller, K.W. Potter and P.R. Wilcock (Editors), *Natural and*
948 *anthropogenic influences in fluvial geomorphology*. Geophysical Monograph Series #89,
949 American Geophysical Union, Washington, D.C., pp. 219-239.

950 Jacobson, R.B., Galat, D.L., 2006. Flow and form in rehabilitation of large-river ecosystems – an
951 example from the Lower Missouri River. *Geomorphology* 77, 249-269.

952 Jacobson, R.B., Gran, K.B., 1999. Gravel sediment routing from widespread, low-intensity
953 landscape disturbance, Current River basin, Missouri. *Earth Surface Processes and*
954 *Landforms* 24(10), 897-917.

955 Jowett I.G., 1997. Instream flow methods: a comparison of approaches. *Regulated Rivers:*
956 *Research and Management* 13, 115-127.

957 Keller, E.A., 1971. Areal sorting of bed-load material: the hypothesis of velocity reversal.
958 *Geological Society of America Bulletin*, 82, 753-756.

959 Kondolf, G.M., 1997. Hungry water: effects of dams and gravel mining on river channels.
960 *Environmental Management* 21(4), 533-551.

961 Kondolf, M., Minner T., 2004. Coarse Sediment Augmentation on the Trinity River Below
962 Lewiston Dam: Geomorphic Perspectives and Review of Past Projects. Report to the Trinity
963 River Restoration Program. University of California, Berkeley.

964 Lane, S.N., Bradbrook, K.F., Richards, K.S., Biron, P.A., Roy, A.G., 1999. The application of
965 computational fluid dynamics to natural river channels: three-dimensional versus two-
966 dimensional approaches. *Geomorphology*, 29(1-2), 1-20.

967 Lane, S.N., Richards, K.S., 1998. High resolution, two-dimensional spatial modelling of flow
968 processes in a multi-thread channel. *Hydrological Processes*, 12(8), 1279-1298.

969 Leclerc M., Boudreault, A., Bechara, J.A., Corfa, G., 1995. Two-dimensional hydrodynamic
970 modeling: a neglected tool in the instream flow incremental methodology. *Transactions of*
971 *the American Fisheries Society* 124, 645-662.

972 Leopold, L.B. Maddock, T., 1953. *The Hydraulic Geometry of Stream Channels and Some*
973 *Physiographic Implications*. United States Geological Survey, Professional Paper 252,
974 Washington, D. C.,USA.

975 Leopold, L.B., Wolman, M.G., Miller, J.P., 1964. *Fluvial Processes in Geomorphology*. W.H.
976 Freeman and Company, San Francisco, Ca, USA.

977 Lisle, T.E., Nelson, J.M., Pitlick J., Madej, M.A., Barkett, B.L., 2000. Variability of bed
978 mobility in natural, gravel-bed channels and adjustments to sediment load at the reach and
979 local scales. *Water Resources Research* 36(12), 3743-3755.

980 Lisle, T E., 1986. Stabilization of a gravel channel by large streamside obstructions and bedrock
981 bends, Jacoby Creek, northwestern California. *Geologic Society of America Bulletin* 97,
982 999-1011.

983 MacWilliams, M.L., Wheaton, J.M., Pasternack, G.B., Kitanidis, P.K., Street, R.L., 2006. The
984 flow convergence-routing hypothesis for pool-riffle maintenance in alluvial rivers. *Water*
985 *Resources Research*. 42, W10427, doi:10.1029/2005WR004391

986 Maddock, I., 1999. The importance of physical habitat assessment for evaluating river health.
987 *Freshwater Biology* 41.

988 McBain, S., Trush, W., 2000. Habitat Restoration Plan for the Lower Tuolumne River. McBain
989 & Trush, Arcata, Ca, USA.

990 McCuen, R.H., 1989. *Hydrologic Analysis and Design*. Prentice-Hall, Inc., Englewood Cliffs.

991 Merz, J.E., Ochikubo Chan, L.K., 2005. Effects of gravel augmentation on macroinvertebrate
992 assemblages in a regulated California river, *River Research and Applications* 21, 61-74.

993 Merz, J.E., Setka, J., Pasternack, G.B., Wheaton, J. M., 2004. Predicting benefits of spawning
994 habitat rehabilitation to salmonid fry production in a regulated California river. *Canadian*
995 *Journal of Fisheries and Aquatic Science* 61, 1433-1446.

996 Miller, A. J., Cluer, B. L., 1998. Modeling considerations for simulation of flow in bedrock
997 channels. In: Wohl, E. E., Tinkler, K.J. (Eds.), *Rivers over rock: fluvial processes in bedrock*
998 *channels*. American Geophysical Union, *Geophysical Monograph Series #107*, Washington,
999 DC, USA, 61-104.

1000 Montgomery, D. R., Buffington, J. M., Smith, R., Schmidt, K., and Pess, G., 1995. Pool spacing
1001 in forest channels, *Water Resources Research*, v. 31, 1097-1105.

1002 Montgomery, D.R., and Buffington, J.M., 1997. Channel-reach morphology in mountain
1003 drainage basins. *Geol. Soc. Am. Bulletin* 109, 596–611.

1004 Montgomery, D.R., Abbe, T.B., Buffington, J.M., Peterson, N.P., Schmidt, K.M., Stock, J.D.,
1005 1996. Distribution of bedrock and alluvial channels in forested mountain drainage basins.
1006 *Nature* 381, 587-589.

1007 Montgomery, D. R., 1999. Process domains and the river continuum, *Journal of the American*
1008 *Water Resources Association* 35, 397-410.

1009 Moyle, P B. and Cech, J.J., 2003. *Fishes: an introduction to ichthyology*, 5th Edition. Prentice
1010 Hall, Englewood Cliffs, NJ, USA.

1011 Negishi, J.N., Inoue, M., Nunokawa, M., 2002. Effects of channelisation on stream habitat in
1012 relation to a spate and flow refugia for macroinvertebrates in northern Japan. *Freshwater*
1013 *Biology* 47(8), 1515-1529.

1014 Newbury, R., Gaboury, M., Bates, D., 1997. Restoring habitats in channelized or uniform
1015 streams using riffle and pool sequences. In: Slaney, P.A., Zaldokas, D. (Eds.), *Fish*
1016 *Rehabilitation Procedures*. British Columbia Ministry of Environment, Lands and Parks,
1017 *Watershed Restoration Technical Circular No. 9*, Vancouver,BC.

1018 Nicholas, A.P., Mitchell, C.A., 2003. Numerical simulation of overbank processes in
1019 topographically complex floodplain environments. *Hydrological Processes*, 17, 727-746.

1020 Parker, G., Toro-Escobar, C.M., Ramey, M., Beck, S., 2003. The effect of floodwater extraction
1021 on the morphology of mountain streams. *Journal of Hydraulic Engineering* 129(11), 885-895.

1022 Pasternack, G.B., Brush, G.S., Hilgartner, W.B., 2001. Impact of Historic land-use change on
1023 sediment delivery to an estuarine delta. *Earth Surface Processes and Landforms* 26, 409-427.

1024 Pasternack, G.B., Wang, C.L., Merz, J., 2004. Application of a 2D hydrodynamic model to
1025 reach-scale spawning gravel replenishment on the lower Mokelumne River, California. *River*
1026 *Research and Applications* 20(2), 205-225.

1027 Pasternack, G.B., Gilbert, A.T., Wheaton, J.M., Buckland, E.M., 2006. Error propagation for
1028 velocity and shear stress prediction using 2d models for environmental management. *Journal*
1029 *of Hydrology*, 328, 227-241.

1030 Poff, N.L., Allan, J.D., Bain, M.B., Karr, J.R., Prestegard, K.L., Richter, B.D., Sparks, R.E.,
1031 Stromberg, J.C., 1997. The natural flow regime. *Bioscience* 47(11), 769-784.

1032 Saldi-Caromile, K., Bates, K., Skidmore, P., Barenti, J., Pineo, D., 2004. Stream habitat
1033 restoration guidelines: final draft. Co-published by the Washington Departments of Fish and
1034 Wildlife and Ecology and the U.S. Fish and Wildlife Service, Olympia, WA, USA.

1035 Singh V.P., 2003. On the theories of hydraulic geometry. *International Journal of Sediment*
1036 *Research* 18(3).

1037 Stalnaker C., 1979. The use of habitat structure preferenda for establishing flow regimes
1038 necessary for maintenance of fish habitat. In: Ward, J. V., Stanford, J. A. (Eds.), *The ecology*
1039 *of regulated streams*. Plenum Press, London, UK.

1040 Stewardson, M.J., McMahon, T.A., 2002. A stochastic model of hydraulic variations within
1041 stream channels. *Water Resources Research* 38(1), 0.1029/2000WR000014.

1042 Surian, N., Rinaldi, M., 2003. Morphological response to river engineering and management in
1043 alluvial channels in Italy. *Geomorphology* 50(4), 307-326.

1044 Thompson, D.M., 2002. Long-Term affect of instream habitat-improvement structures on
1045 channel morphology along the Blacklegde and Salmon Rivers, Connecticut, USA.
1046 Environmental Management 29(1), 250-265.

1047 Thompson, S.M., Campbell, P.L., 1979. Hydraulics of a large channel paved with boulders.
1048 Journal of Hydraulic Research 17(4), 341-355.

1049 Thompson, D.M., Stull, G.N., 2002. The development and historic use of habitat structures in
1050 channel restoration in the United States: the grand experiment in fisheries management.
1051 Geographie Physique et Quaternaire 56(1), 45-60.

1052 Thompson, D.M., Nelson, J.M., Wohl, E.E., 1998. Interactions between pool geometry and
1053 hydraulics. Water Resources Research 34, 3673-3681.

1054 U.S. Fish Wildlife Service (USFWS)., 1999. Trinity River Flow Evaluation. Department of the
1055 Interior, Washington, DC, USA.

1056 U.S. Fish Wildlife Service (USFWS)., 2002. Mainstem Trinity River chinook salmon spawning
1057 survey year 2000 and 2001. Department of the Interior, Washington, DC, USA.

1058 Van Asselt, M. B. A., Rotmans, J., 2002. Uncertainty in integrated assessment modelling - From
1059 positivism to pluralism. Climatic Change 54, 75-105.

1060 Webb, R. H., Schmidt, J. C., Marzolf, G. R., Valdez, R. A., 1999. The controlled flood in Grand
1061 Canyon. Geophysical Monograph Series #110, American Geophysical Union, Washington,
1062 D.C.

1063 Wheaton, J. M., Pasternack, G. B., Merz, J. E., 2004a. Spawning habitat rehabilitation - 1.
1064 conceptual approach & methods. International Journal of River Basin Management 2(1), 3-
1065 20.

1066 Wheaton, J.M., Pasternack, G.B., Merz, J.E., 2004b. Spawning habitat rehabilitation - 2. using
1067 hypothesis development and testing in design, Mokelumne River, California, U.S.A.
1068 International Journal of River Basin Management 2(1), 21-37.

1069 Wheaton, J. M., Pasternack, G. B., Merz, J. E., 2004c. Use of habitat heterogeneity in salmonid
1070 spawning habitat rehabilitation design. In: de Jalón Lastra, D. G., Martínez, P. V. (Eds.),
1071 Fifth International Symposium on Ecohydraulics: Aquatic Habitats: Analysis and
1072 Restoration, IAHR-AIRH, Madrid, 791-796.

1073 Wilcock, P. 2004. Draft Sediment Budget and Monitoring Plan, Trinity River, California,
1074 Lewiston Dam to Douglas City. Johns Hopkins University, Report to the Trinity River
1075 Restoration Program, Baltimore.

1076 Wilcock, P.R., Barta, A.F., Shea, C.C., Kondolf, G.M., Matthews, W.V.G., Pitlick, J.C., 1996.
1077 Observations of flow and sediment entrainment on a large gravel-bed river. Water Resources
1078 Research 32, 2897-2909.

1079 Wilcock, P.R., Kenworthy, S.T. Crowe, J.C., 2001. Experimental study of the
1080 transport of mixed sand and gravel. Water Resources Research 37(12), 3349-3358.

1081 Williams, G.P. Wolman, M.G., 1984. Downstream Impacts of Dams on Alluvial Rivers. United
1082 States Geological Survey, Professional Paper 1286, Washington, DC, USA.

1083 Wolman, M. G., 1954. A Method of Sampling Coarse River Bed Material. Transactions of the
1084 American Geophysical Union 35(6), 951-956.

1085

1086

1087

1088

1089 **10. List of Figures**

1090

1091 Figure 1. Regional map showing Trinity River basin, major impoundments, and the Lewiston
1092 hatchery reach.

1093 Figure 2. Annual peak discharge hydrograph for Trinity River at Lewiston, CA illustrating
1094 impact of flow regulation.

1095 Figure 3. Aerial photographs of LHR showing natural and anthropogenic boundary controls in
1096 (A) 1944 and (B) 1998.

1097 Figure 4. Photographs of primary boundary controls in LHR, including (A) hatchery and valley
1098 confinement and (B) artificial riffle-weirs.

1099 Figure 5. Topographic map of study reach showing cross section locations.

1100 Figure 6. Grain size distributions showing affect of armoring on bed texture.

1101 Figure 7. Longitudinal bed and water surface profiles demonstrating the controlling effect of
1102 artificial rock-weir riffles on channel hydraulics.

1103 Figure 8. At-a-station velocity hydraulic geometry plot demonstrating the lack of a “velocity
1104 reversal” in any of the LHR riffle-pool units.

1105 Figure 9. Validation cross sections comparing 2D model predictions with field measurements.

1106 Figure 10. 2D model depth results at (A) 8.5, (B) 13, (C) 71, and (D) 170 m³/s.

1107 Figure 11. 2D model velocity results at (A) 8.5, (B) 13, (C) 71, and (D) 170 m³/s.

1108 Figure 12. Joint distribution of depth and velocity for (A) 8.5, (B) 13, (C) 71, and (D) 170 m³/s.

1109 Figure 13. 2D model Shields stress results for (A) 8.5, (B) 13, (C) 71, and (D) 170 m³/s.

1110 Figure 14. Distribution of sediment transport regimes in the study reach as a function of
1111 discharge.

1112 Figure 15. 2D model GHSI results for chinook salmon life stages. (A) spawning without SHSI,
1113 (B) spawning with SHSI, (C) juvenile, and (D) fry. Darker shading indicates higher quality
1114 habitat.

1115 Figure 16. Relation between the percent of channel predicted to be at least “medium” quality
1116 habitat (GHSI > 0.4) and discharge.

1117

Figure 1

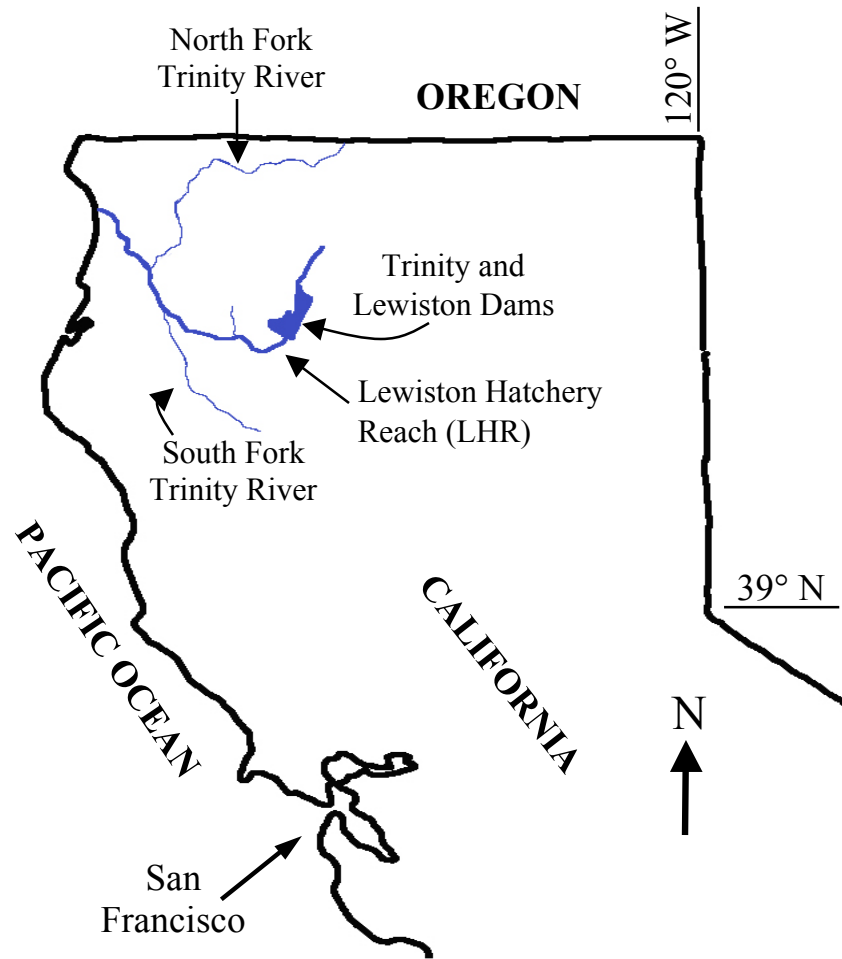
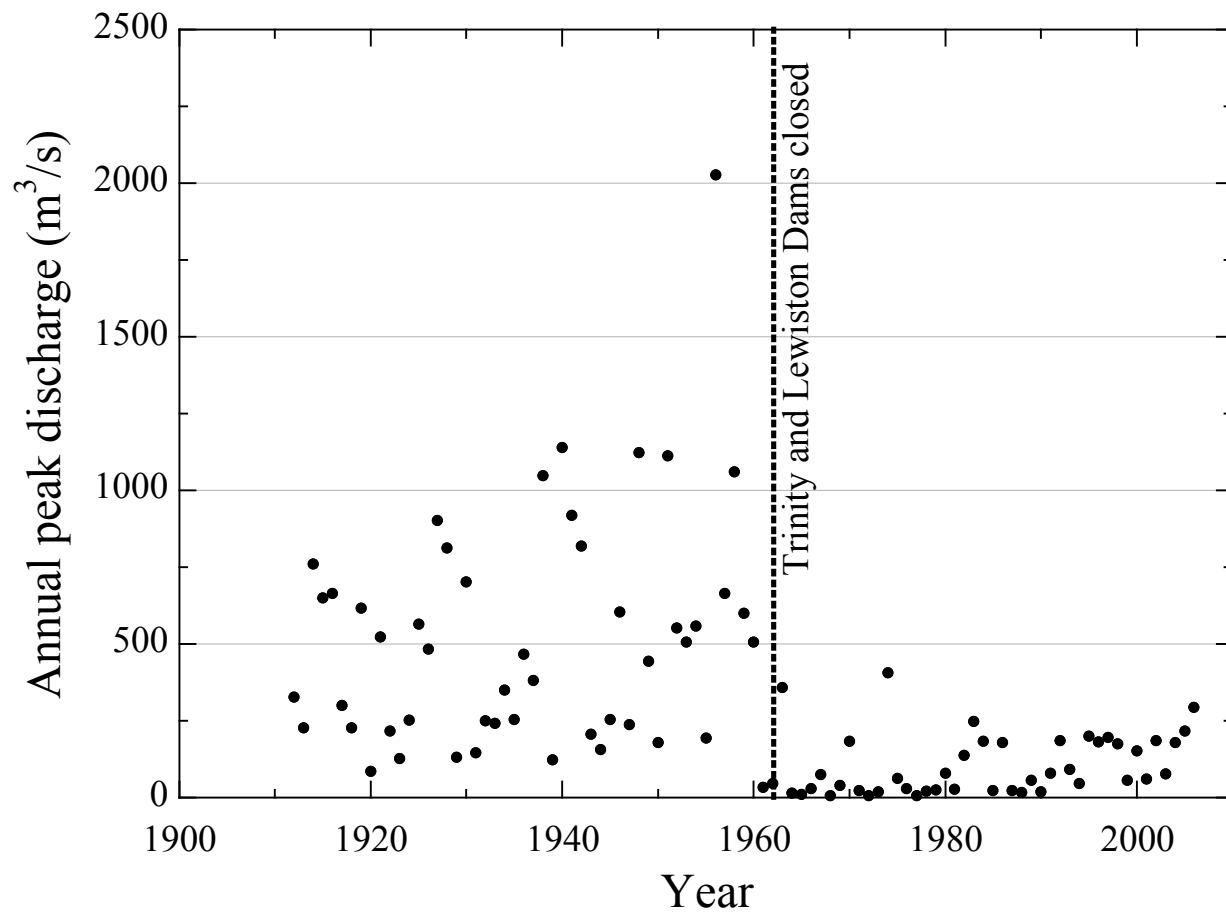


Figure 2



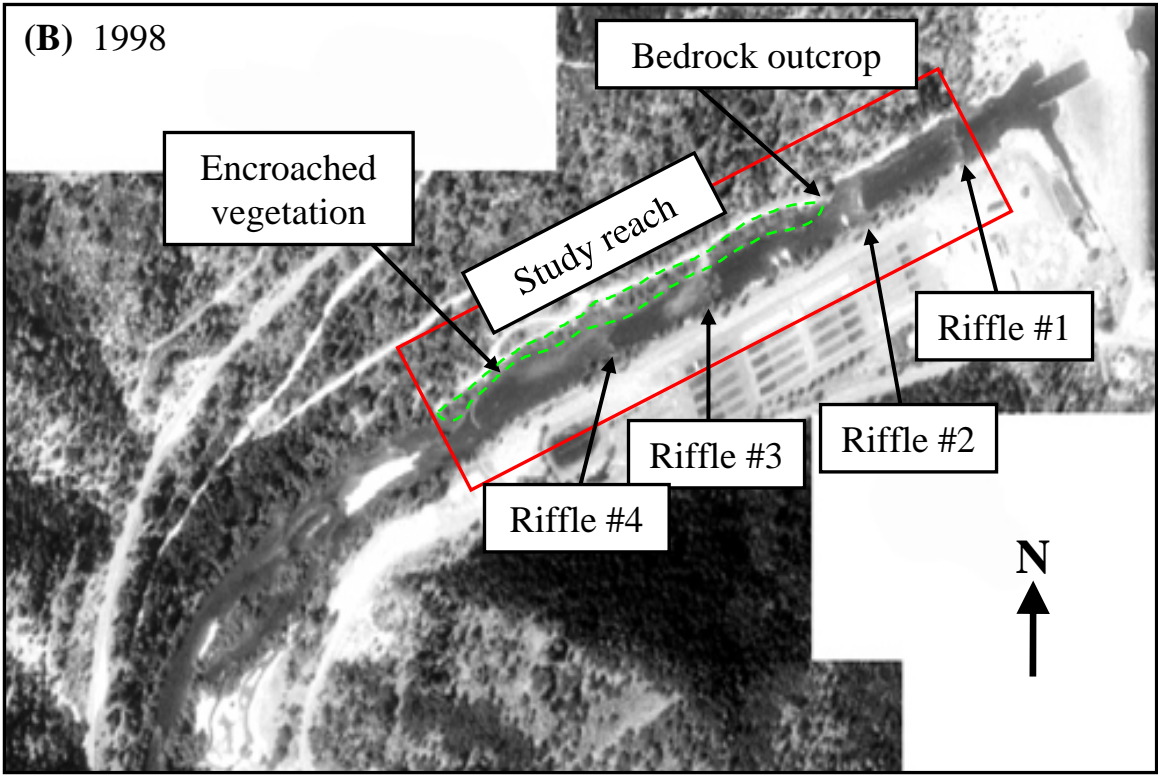
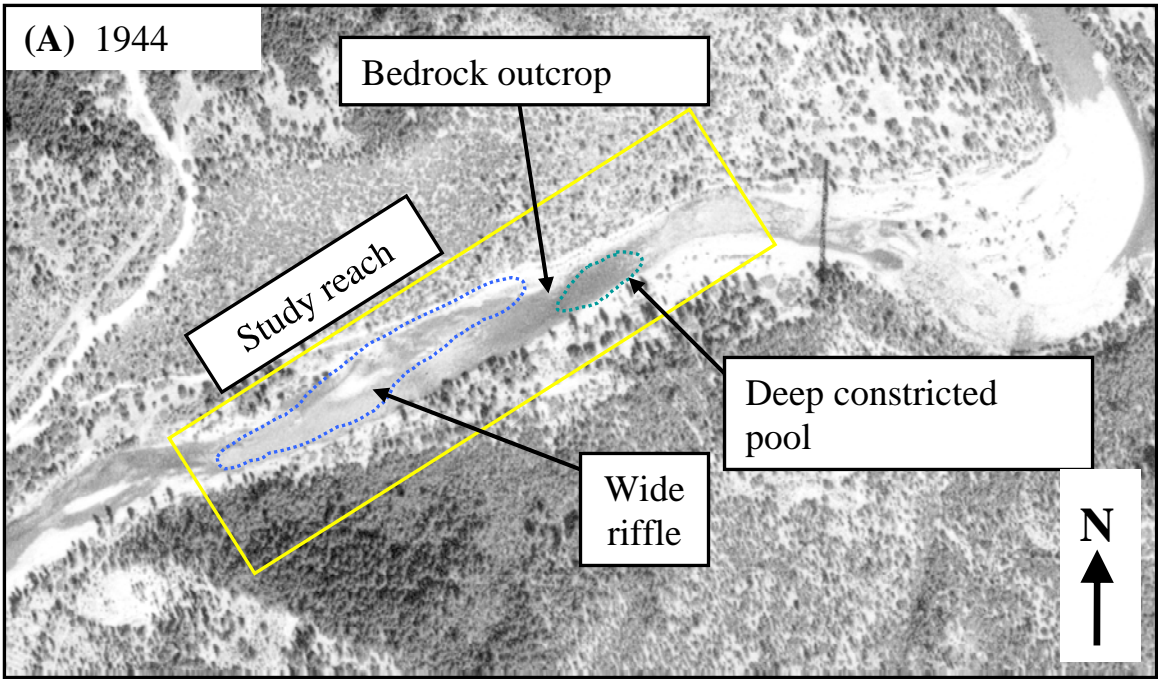


Figure 4



Figure 5

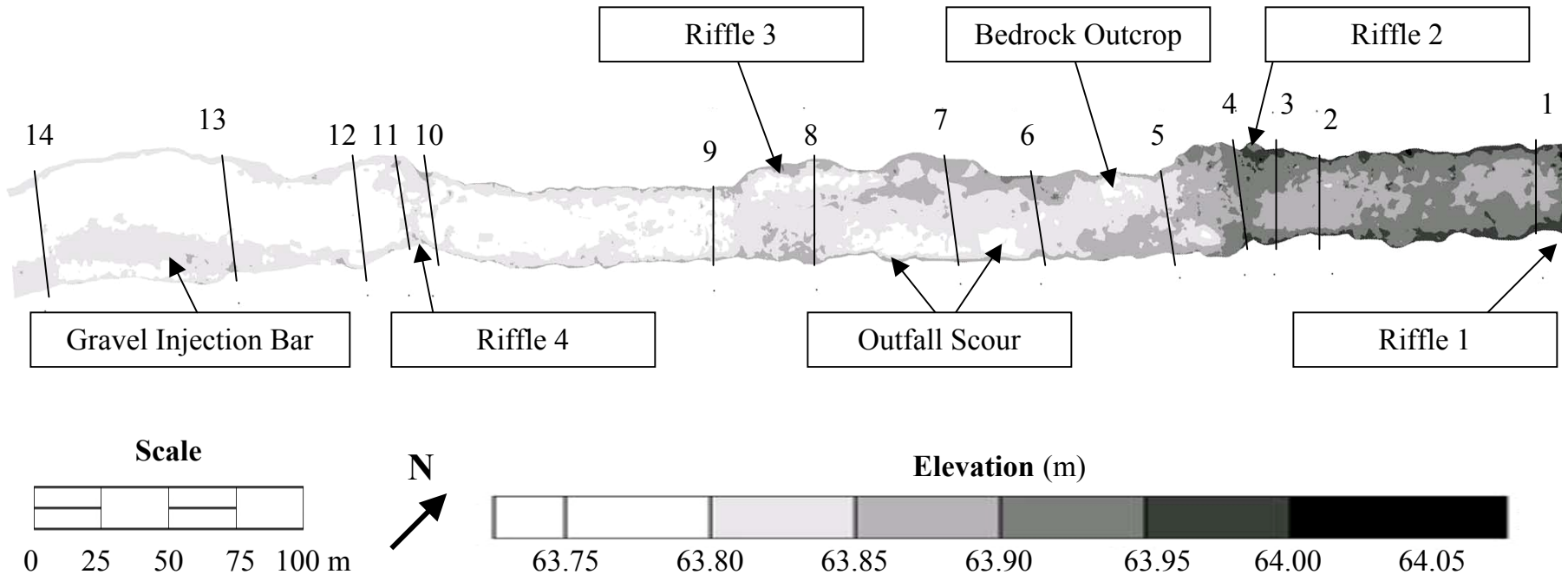


Figure 7

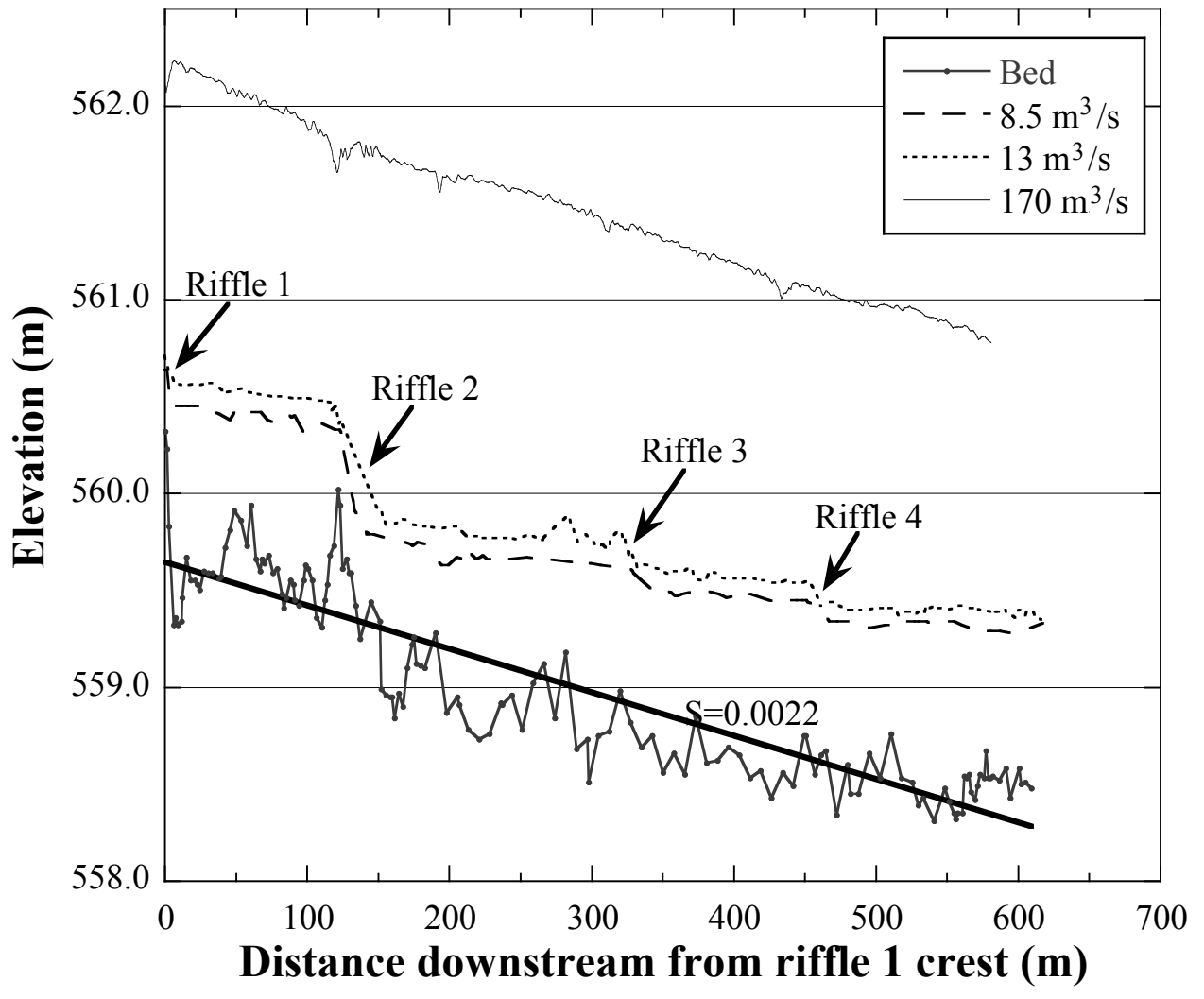


Figure 8

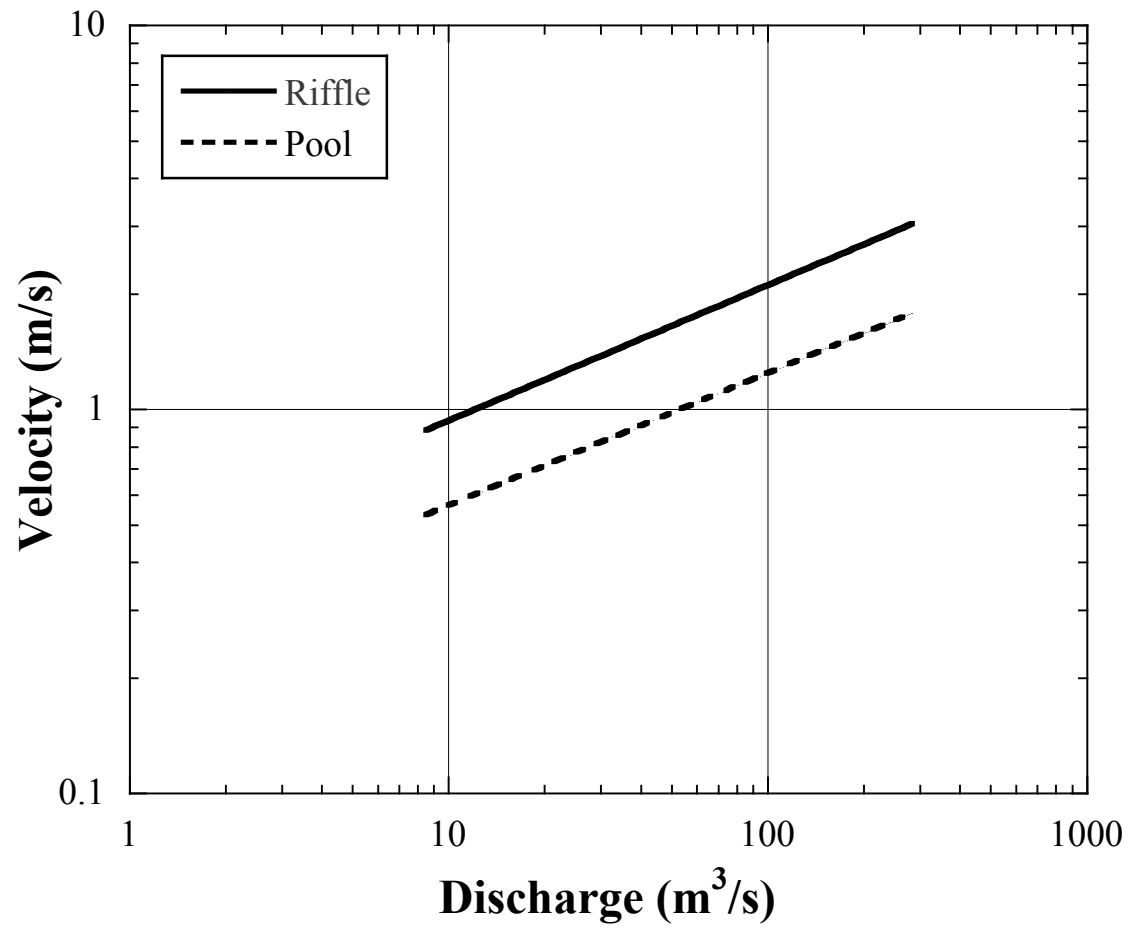
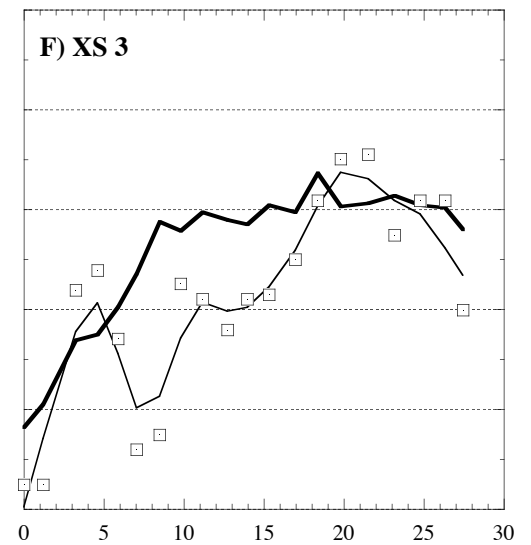
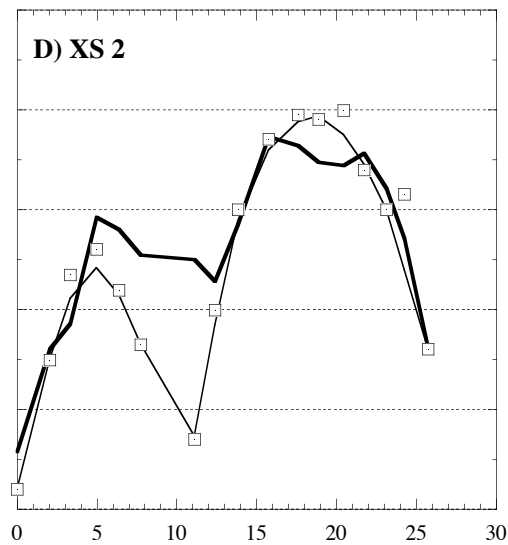
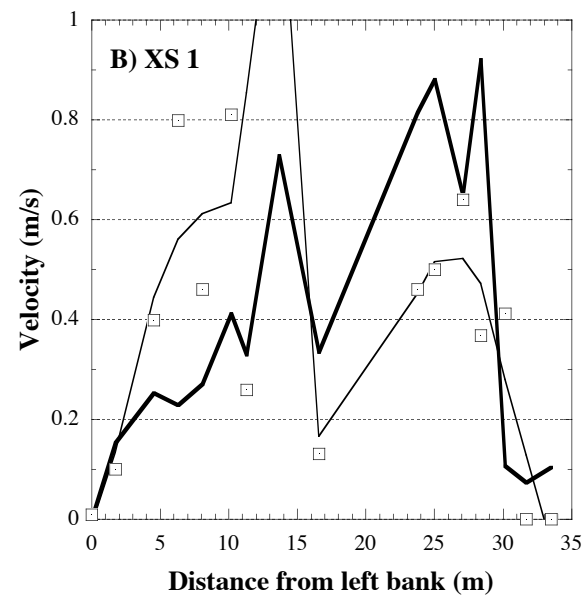
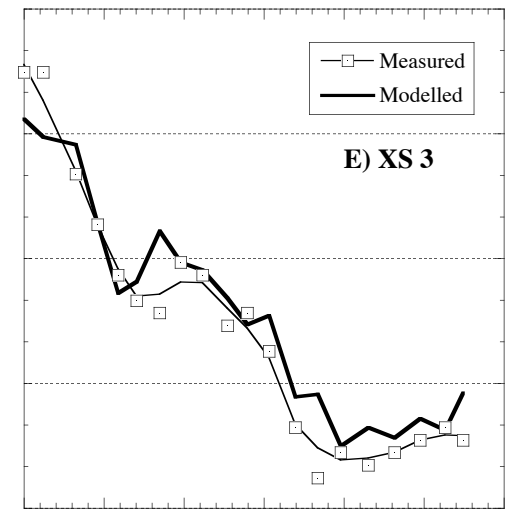
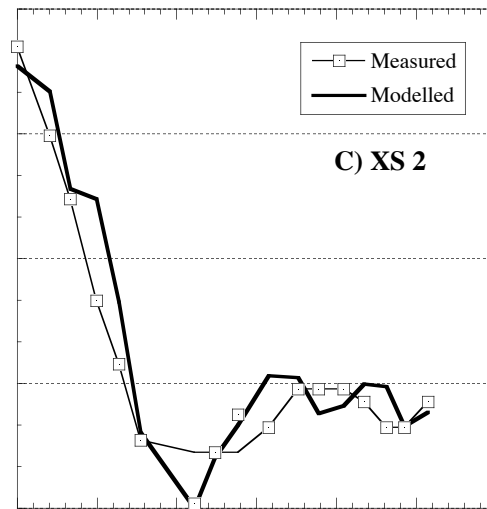
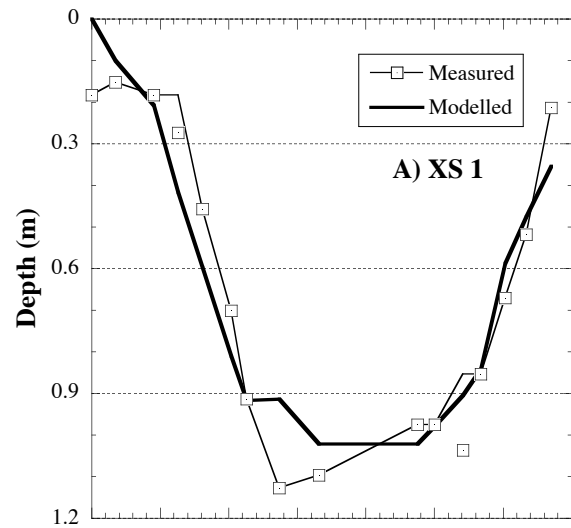


Figure 9



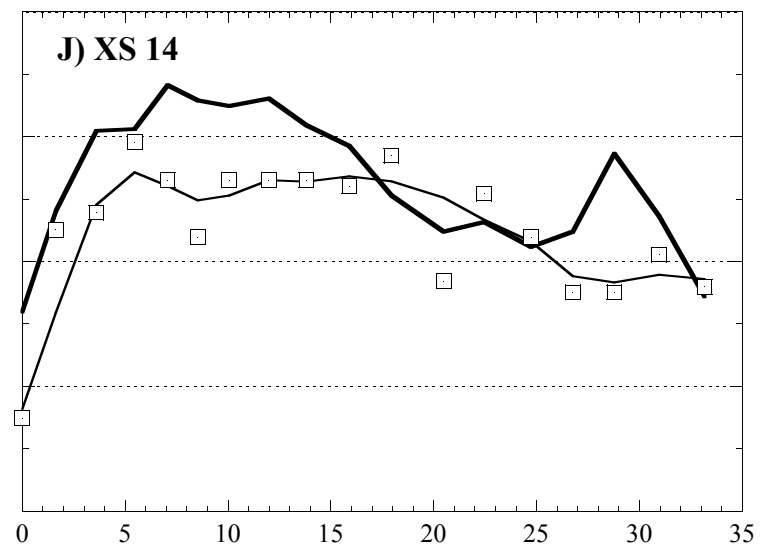
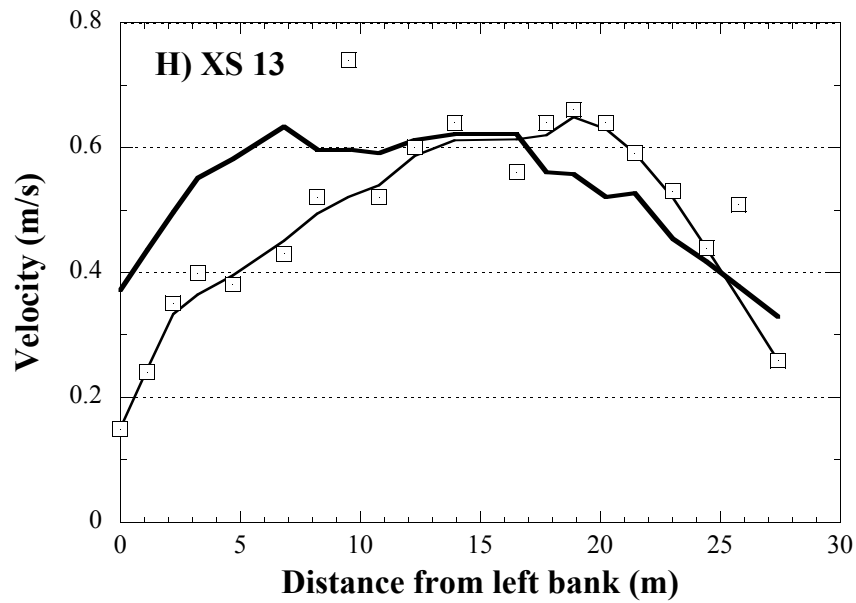
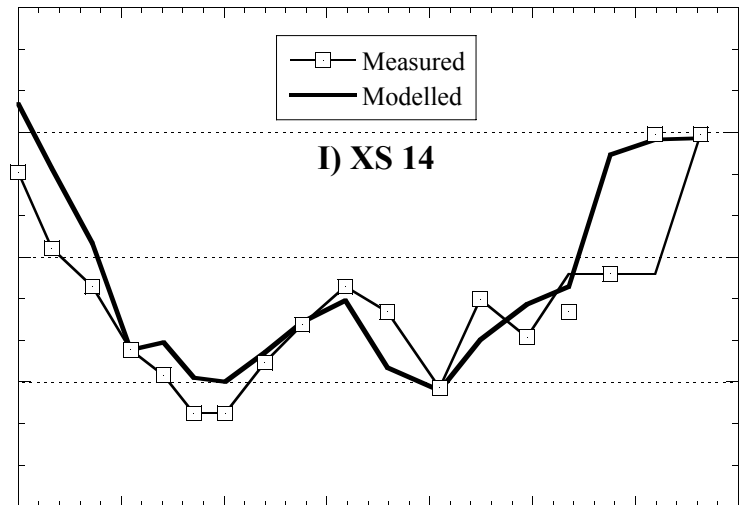
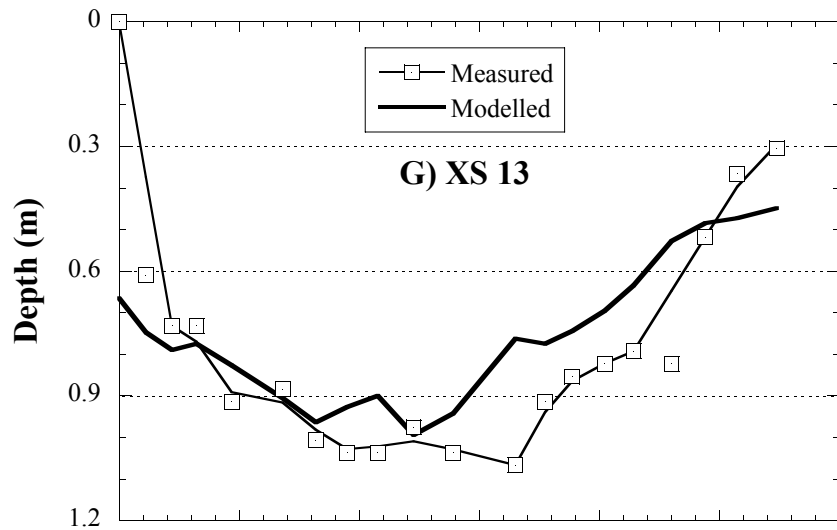


Figure 10

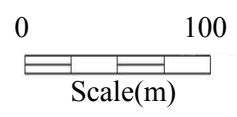
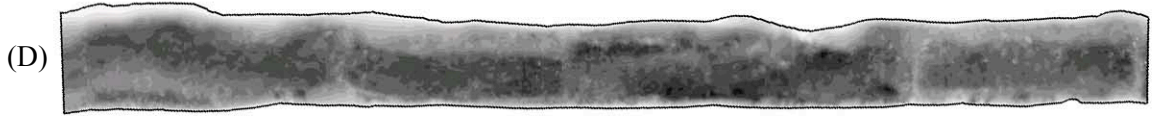
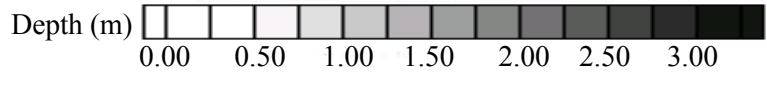
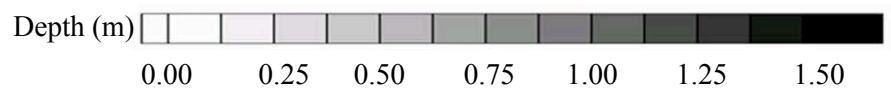
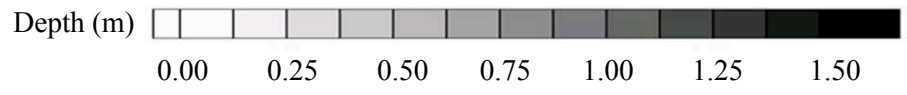
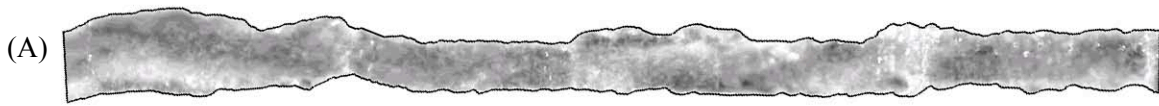
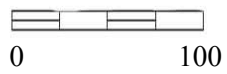
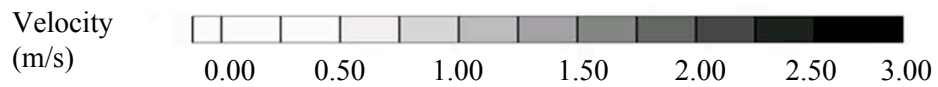
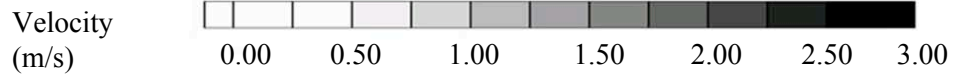
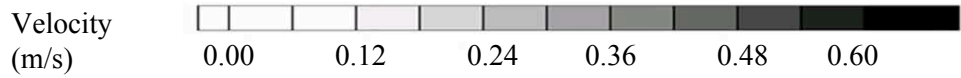
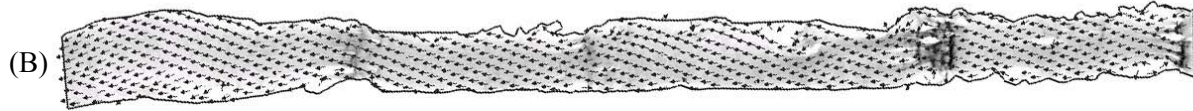
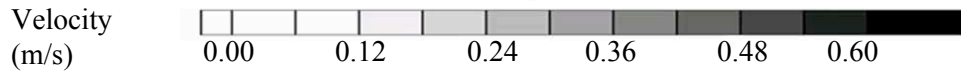
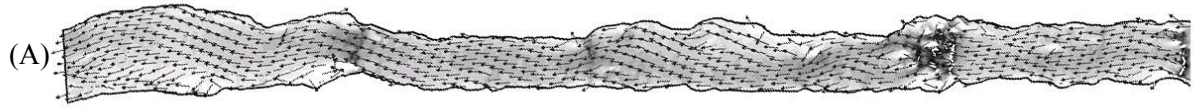
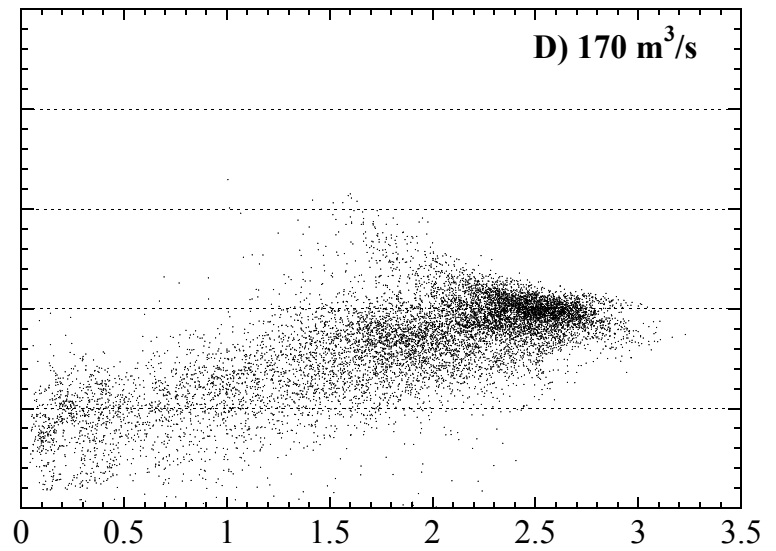
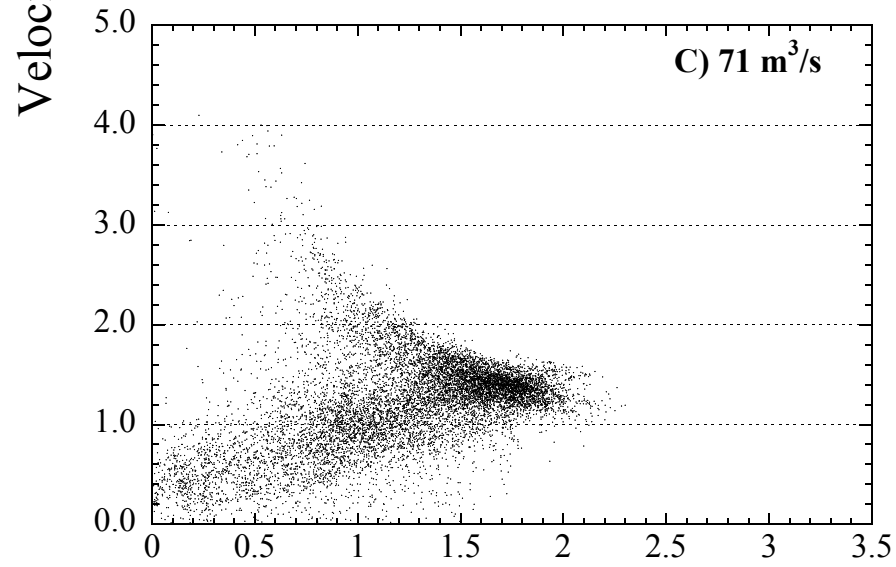
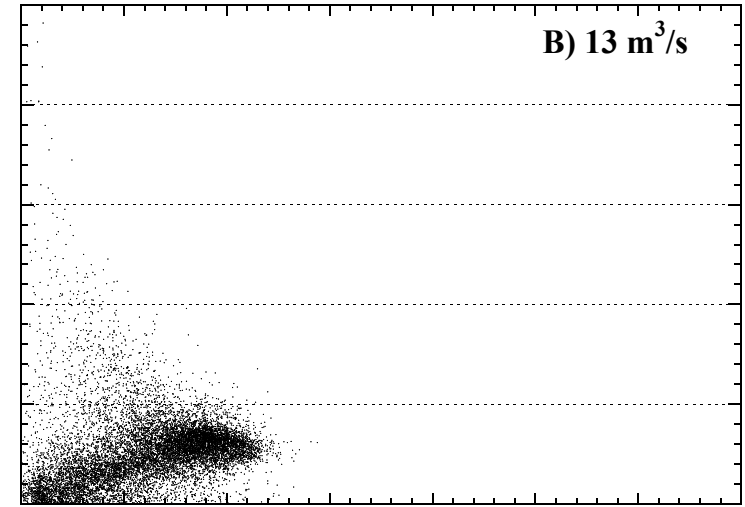
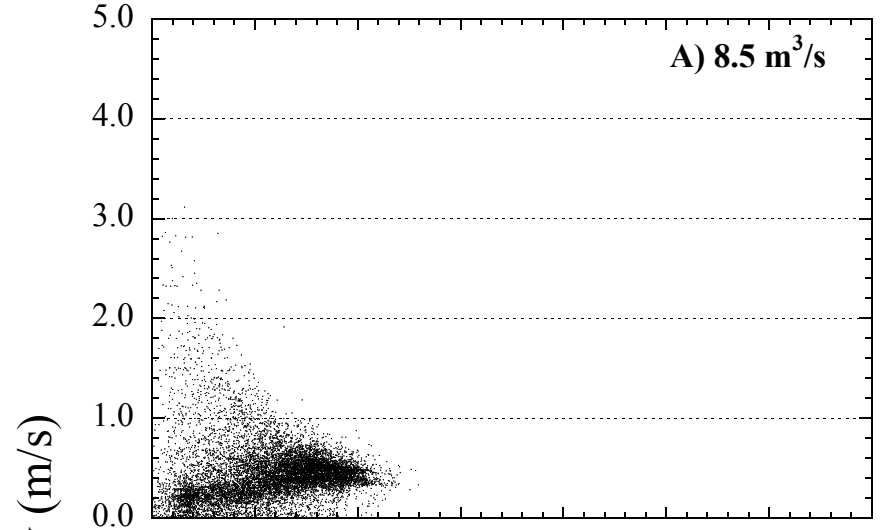


Figure 11



Scale (m)





Depth (m)

Figure 13

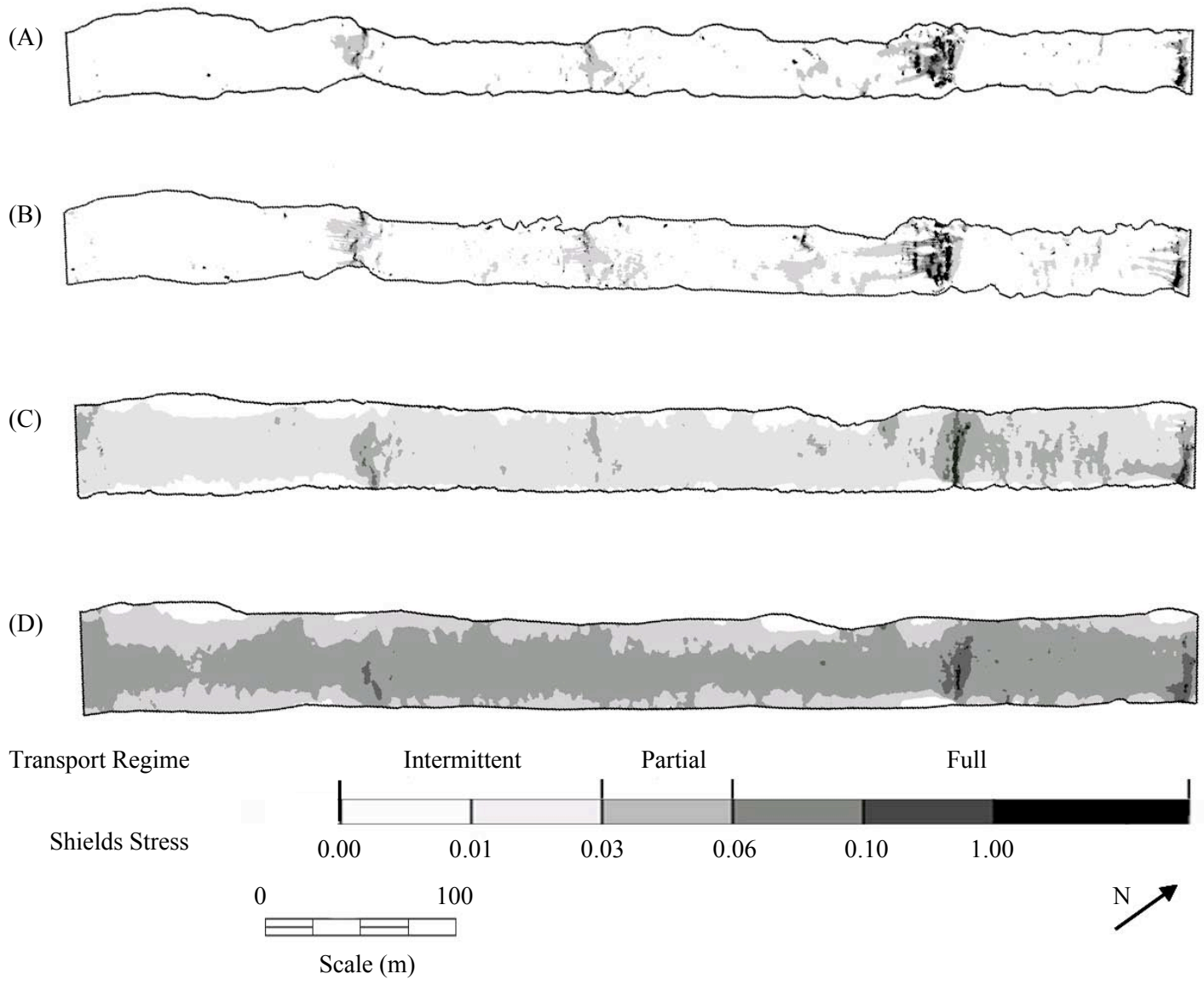


Figure 14

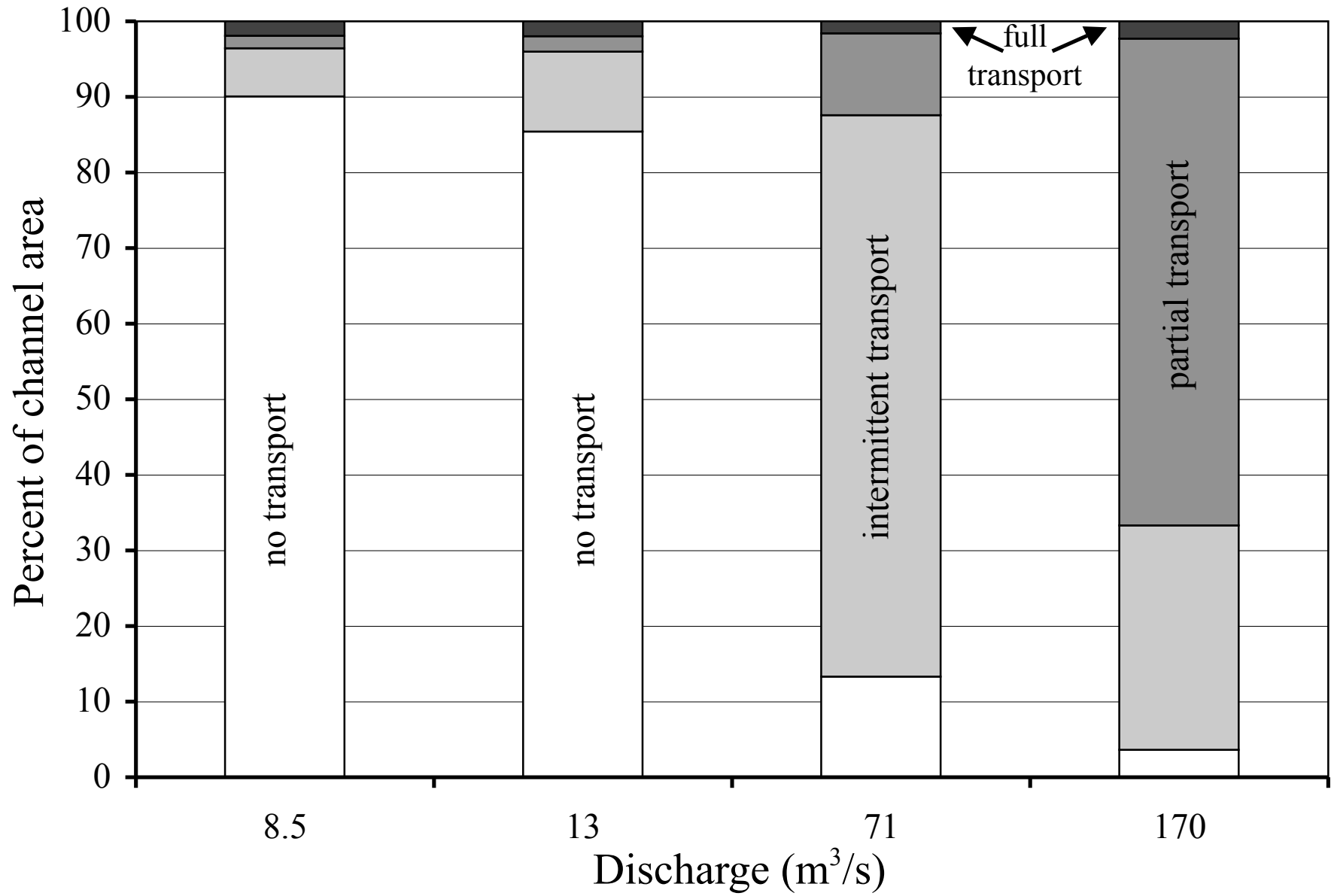
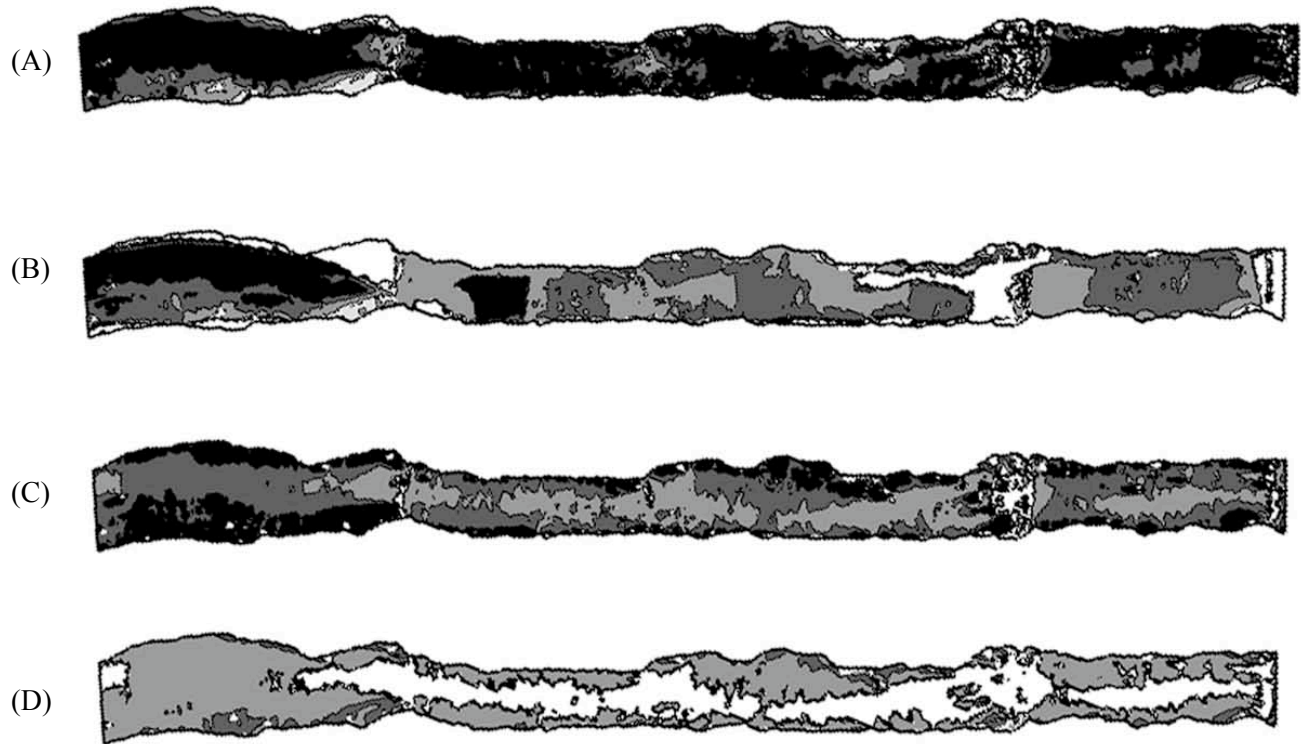


Figure 15



Habitat quality

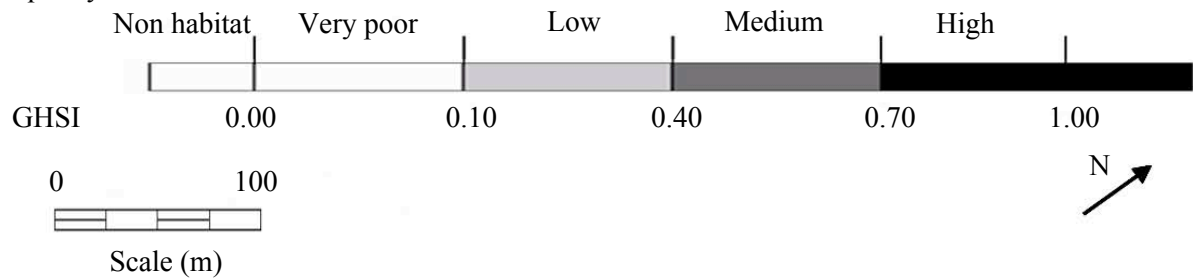


Figure 16

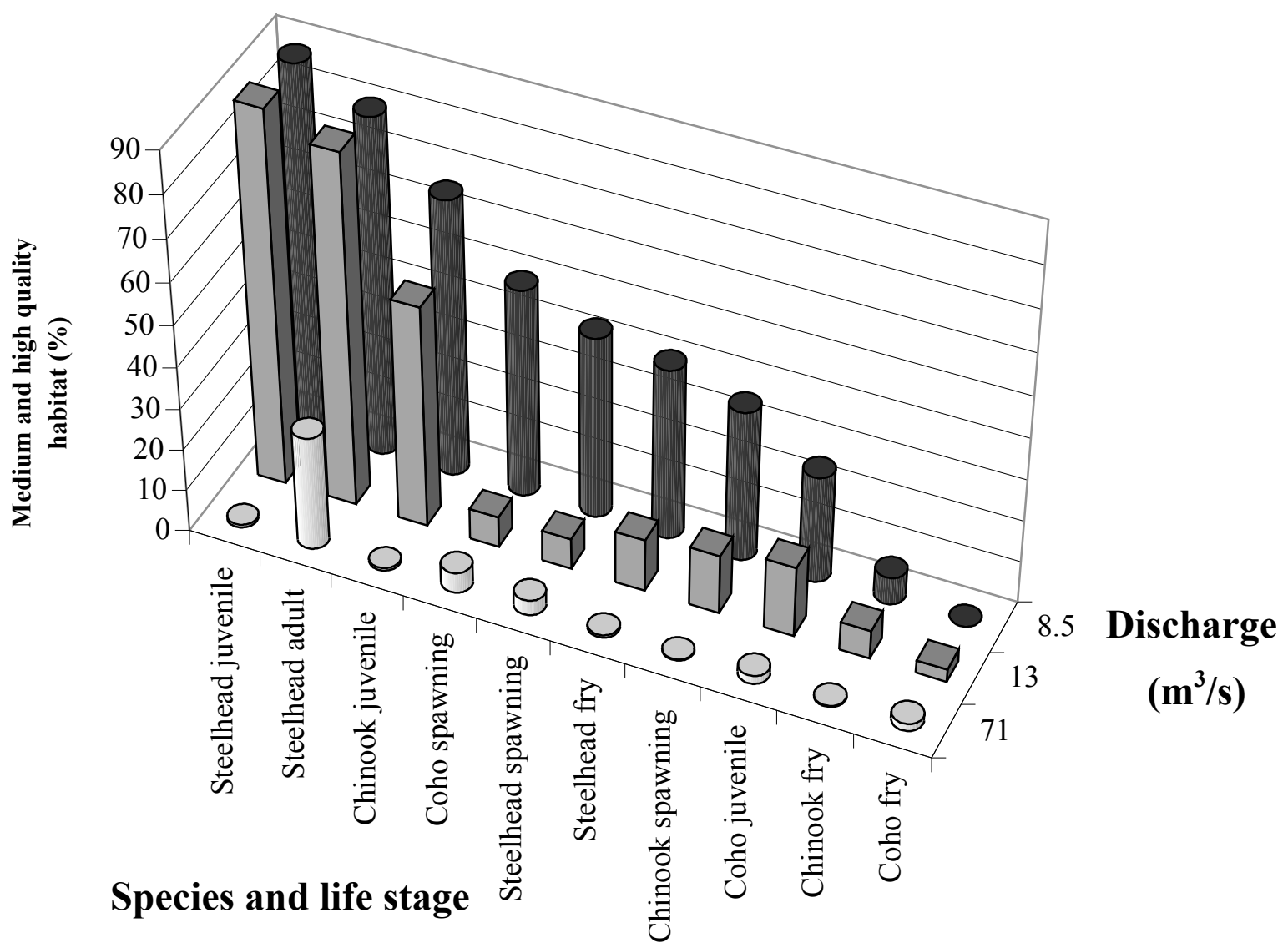


Table 1
Characterization of Physical Controls on Fluvial Environments

	Natural	Anthropogenic
Boundary Controls	Valley confinement (H, G, R)	Bank stabilization (H, G, R)
	Bedrock outcroppings (H,G, R)	Armoring (G)
	Boulders (H,G)	Levees (G, R)
	Large woody debris (H, G)	In-stream habitat improvement (H, G)
	Bed material size (H, G)	Woody debris removal (H, G)
	Dense vegetation (H, G, R)	
Input Controls	Geology/soils (B)	Land use (R, B)
	Climate (B)	Dams (R, B)
	Topography (B)	Diversions (R, B)
	Land cover (R, B)	

Letters denote spatial scales: H is Hydraulic Unit (0.1-1 channel widths), G is Geomorphic Unit (10 channel widths), R is Reach Unit (100-1000 channel widths), B is Basin.

Table 2
Hydraulic geometry exponent values associated with eqs. 1-3.

Cross section	Geomorphic unit	b	f	m
1	Riffle Exit	0.13	0.52	0.36
2	Pool	0.11	0.54	0.35
3	Pool Exit	0.11	0.55	0.34
4	Riffle	0.08	0.55	0.37
5	Riffle Exit	0.18	0.49	0.33
6	Pool	0.11	0.53	0.35
7	Pool	0.17	0.50	0.33
8	Pool Exit	0.16	0.50	0.33
9	Riffle Exit	0.20	0.48	0.32
10	Riffle	0.17	0.50	0.33
11	Riffle	0.12	0.53	0.35
12	Riffle Exit	0.22	0.47	0.31
13	Pool	0.17	0.49	0.34
14	Pool exit	0.51	0.28	0.21
	Average	0.17	0.50	0.33
	Standard Deviation	0.10	0.07	0.04